2018年 8月

博士學位論文

A Study on the DC-DC Boost Type Converter using Switched-Inductor

朝鮮大學校 大學院

電 氣 工 學 科

吳 晩 惜

2018年 8月 博士學位論文 A Study on the DC-DC Boost Type Converter using Switched-Inductor 吳 晩 惜

2018年 8月

博士學位 論文

A Study on the DC-DC Boost Type Converter using Switched-Inductor

朝鮮大學校 大學院

電 氣 工 學 科

吳 晩 惜

A Study on the DC-DC Boost Type Converter using Switched-Inductor

스위치드 인덕터를 이용한
DC-DC 부스트 컨버터에 관한 연구

2018年　8月 24日

朝鮮大學校 大學院

電氣工學科

吳　晩　惜

A Study on the DC-DC Boost Type Converter using Switched-Inductor

指導敎授 曺 錦 培

이 論文을 工學博士學位 申請論文으로 提出함

2018年 4月

朝鮮大學校 大學院

電氣工學科

吳 晩 惜

吳晩惜의 博士學位 論文을 認准함

委員長 朝鮮大學校 教授 金南勳 (印)

委 員 全南科學大學校 教授 金大坤 (印)

委 員 朝鮮大學校 教授 崔然王 (印)

委 員 朝鮮大學校 教授 Nguyen Minh Khai (印)

委 員 朝鮮大學校 教授 曺錦洽 (印)

2018年 6月

朝鮮大學校 大學院

Contents

List of Tables

List of Figures

ABSTRACT

스위치드 인덕터를 이용한 DC-DC 부스트 컨버터에 관한 연구

Oh Man-Seok
Advisor : Prof. Cho Geum-Bae, Ph.D.
Department of Electrical Engineering
Graduate School of Chosun University

기존 낮은 DC입력을 높은 DC로 승압하는 DC-DC 부스트 컨버터는 전력용 반도체 스위칭 소자의 고전압 스트레스와 연속 전류 모드에서 작동하는데 필요한 큰 인덕턴스로 인해 고 이득 DC-DC 변환 응용에는 적합하지 않았다. 하지만, 최근에는 고 이득 DC-DC 부스트 컨버터의 필요성 증가와 기존의 부스트 컨버터를 개선하는 다양한 연구 방법이 제시되고 있어 많은 연구자들의 주요 토픽으로 연구를 수행하고 있다.

본 논문에서는 새로운 고 이득 DC-DC 부스트 컨버터를 제안하고 이를 고찰하고자 한다. 제안 된 고 이득 DC-DC 부스트 컨버터 구조는 변압기를 사용하지 않고 낮은 입력 전압 기반의 토폴로지 구성으로 전력용 반도체 스위치 및 커패시터의 전압 스트레스를 감소시킬 수 있으며 높은 전압 이득을 얻을 수 있는 장점을 가지고 있다. 이러한 제안된 고 이득 DC-DC 부스트 컨버터 토폴로지는 가변적인 저전압 입력 전압이 높은 안정화 된 DC 출력 전압으로 변환되는 고 이득 변환의 응용에 적합하다. 따라서 본 논문에서는 고 이득을 얻기 위하여 하나의 스위치드 인덕터 단위 셀 방식을 기반으로 두개의 스위치드 인덕터 셀 방식 및 다중 스위치드 인덕터 셀로 확장이 가능한 새로운 고 이득 DC-DC 부스트 컨버터를 제안하고 이론적 고찰, 동작원리,

CCM과 DCM 회로해석 및 수동 부품 선택에 대한 지침을 제시하였다. 제안된 방식의 이론적 타당성을 검증하기 위해 400 V 출력 전압과 800 W의 시스템을 대상으로 폐루프 제어기에 대한 동적 응답 특성을 PSIM 시뮬레이션 툴을 사용하여 수행하였다. 또한 제안 된 고 이득 DC-DC 부스트 컨버터의 실험을 위한 프로토 타입을 제작하였으며 PWM 방식을 구현하기 위해서는 Texas Instruments의 DSP TMS320F28035 kit을 사용하여 제안 된 새로운 고 이득 DC-DC 부스트 컨버터의 이론적 분석과 계산식을 검증하기 위한 실험을 수행하여 입증하였다.

Ⅰ. Introduction

A. Motivation

Recently, the power demand is significantly rising due to population increase and the significant industrialization. However, using fossil fuels such as oil, coal and natural gases to generate electricity causes environmental pollution problems. Besides that, fossil fuels are difficult to gratify the demand for electricity. Therefore, using and development of the green energy sources [1]-[15] is a constructive approach. Solar energy is pollution free and freely available everywhere. Furthermore, solar cells directly converts solar energy into electrical energy. The sunlight can be converted into electrical energy by using photovoltaic cells. Fuel cell directly converts the chemical energy into electrical energy. Fuel cells has been developed to supersede the accumulators and batteries. These green energy sources has many benefit, i.e. its cheap, scale flexibility, pollution free, clean and little maintenance. However, the output voltage of green energy sources is relatively low and instability.

Recently, power electronics has developed significantly, which has two major topics. The first topic is the development of power semiconductor component that are high voltage capability, high speed and high power applications. The other is focused real-time controller systems that can improve advanced and complex control methods. So, the power conversion systems have been attracting many attentions of researchers in scientific and industrial research. The power conversion system is insert into between input DC source such as battery, PV or FC and residential loads such as load DC, dc-ac inverter to achieve higher DC voltage as shown in Fig. 1-1.

In the model of green energy source system as shown in Fig. 1-1, we can see that to bring power from the source to the load, we have to pass dc-dc power converter. The power converter has many functions such as boost voltage, voltage stabilizer, etc. There are many DC loads such as phones, computers, DC motors or LED lighting, and etc. The DC loads required a different voltage level to operate. So, dc-dc converters is used to generate the desired DC voltage from the low dc output voltage of this green energy source to provide up to DC load. In addition to DC loads, this power converter is also a power source for dc-ac inverters. In this case, to generate the desired ac voltage, the power converter have to produce a high DC bus voltage for example 400V for one phase system and 600V for three phases system from the low dc output voltage of this green energy source. And then, a dc-ac inverter will invert the high DC bus voltage into a single phase or three phase AC voltage. Recently, many dc-dc converters have been proposed and consider to achieve a high DC bus voltage with two basic configurations that are non-isolated and isolated. In isolated configurations [16]-[20], transformers are used to generate a desired voltage by adjusting the turn ratio of transformer.

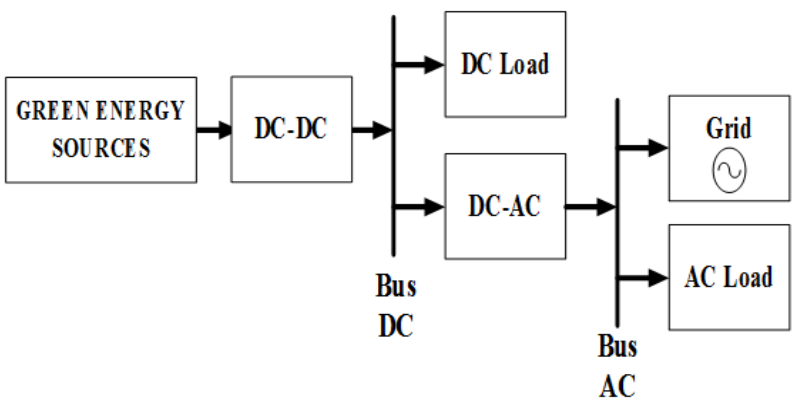

Fig. 1-1 Model of green energy source system

As a results, voltage again is significantly improved. Also, voltage stress across the component is limited. However, with using Transformer leads to size and cost of system and low efficiency. In non-isolated configurations, a conventional dc-dc boost converter [21] as shown in Fig. 1-2 is inserted into between input DC sourced and inverter to achieve higher voltage to converter power which connected to the grid.

Fig. 1-2 shows the simplest dc-dc boost converter. However, the conventional dc-dc boost converter is not suitable for high step-up conversion applications. The other demerits of conventional dc-dc boost converter are high voltage stress across power semiconductor and a large inductance that is required to guarantee operating in continuous conduction mode. The dc-dc boost converters are used in [22]-[25] to provide a high voltage with a moderate duty cycle. In [26]-[36], a high gain transformerless converter was introduced. It is a combination of two-level dc-dc converters. As a result, a large number of components was used and it results in an increase in expense.

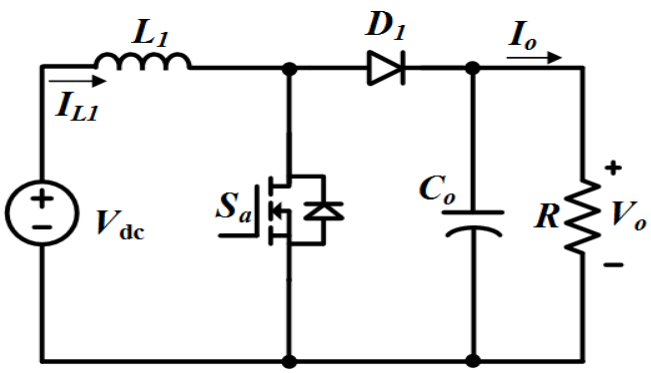

Fig. 1-2 Conventional dc-dc boost converter

In order to improve high voltage gain switched capacitor techniques and switched inductor were also discussed [37]-[46]. But the demerit was that the high charging current will flowing through power semiconductor. As a result, the conduction losses increased significantly.

In this study, a new high gain dc-dc boost type converter is proposed. The introduced converter is composed of two inductors, six diodes, two active-switches, and two capacitors. The introduced inverter is applicable to photovoltaic or fuel cells applications that need a high voltage gain ratio. The circuit analysis, operating principles and simulation results of the high gain dc-dc boost type converter are presented. Also, a guideline of passive components selection for the introduced topology is illustrated. Simulation results in PSIM software with 400 V output voltage and 800 W output power are shown to verify the theoretical analysis. Finally, the experimental results of the proposed novel high gain dc-dc boost type converter are also indicated to prove calculated equations and theoretical analyses

B. Scope of the dissertation and organizations

The objective of this study is investigated on the development of boost converter power structures. And then, discussing a high gain dc-dc boost type converter to provide a high voltage gain ratio for photovoltaic or fuel cells applications. Based on proposed topology, a extended circuit of proposed topology is discussed to increase voltage gain of the converter. Discussing passive components selection for high gain dc-dc boost type converter to provide a high performance.

The dissertation is organized as follows:

- Chapter 1 is an introduction to some of the previous research in high boost converter based on a review of current literature.
- In chapter 2, a discussion of isolation configuration topologies is provided. In isolation configuration, Several power converters such as flyback and forward topology, push-pull topology and the conventional current-fed full bridge topology are discussed and compared. Besides that, the operating principle and the control scheme of non-isolation configuration topologies such as boost dc-dc converter topology, buck dc-dc converter topology, buck-boost dc-dc converter topology, interleaved boost converter topology and high step-up stacked dc-dc converter topology is also presented in chapter 2. Furthermore, the PWM methods for non-isolation topology and isolation topology are discussed.
- In chapter 3, the fundamental idea of the high gain boost converter topology is presented. The structure of proposed high gain dc-dc boost type converter is introduced in this chapter. The operating principle and circuit analysis of proposed high gain dc-dc boost type converter in both continuous conduction mode and discontinuous conduction mode are presented. Furthermore, the proposed phase shift PWM control strategy for proposed high gain dc-dc boost type converter is discussed in detail.

- In chapter 4, an extended circuit topology for proposed converter is illustrated. The operating principle and circuit analysis of proposed extended converter using 2-switched-inductor cells are also presented. A comparison of voltage gain with using n-switched-inductor cells is discussed in this chapter. Moreover, the guidelines for passive components design of proposed converter is presented.
- Chapter 5 presents the simulation and experimental results of the proposed converter. Simulation results of proposed converter using 1-switched-inductor cell with G=8 and G=4 are presented and compared to calculation results in this chapter. Also, simulation results of proposed converter using 2-switched-inductor cells with G=16 are presented and compared to calculation results. Furthermore, dynamic performance of proposed converter in simulation are also shown in this chapter. In experiment, the experiment prototype of the proposed high gain dc-dc boost type converter was developed based on kit TMS320F28035 (i.e., clocked at frequency of 60 MHz) of Texas Instruments to implement the PWM scheme. Experimental results of proposed converter using 1-switched-inductor cell with G=8 and G=4 are presented and compared to simulation and calculation results. The dynamic performance of proposed high gain dc-dc boost type converter when G=8 are presented in this chapter.
- Chapter 6 summarizes the research work included in this dissertation and gives future research directions.

Ⅱ. DC-DC Converter Topology Surveys

A. Isolation configuration

A high-frequency transformer (pulse transformer) is added to isolate the input and output of the transformer. The high-frequency transformer can operate with around few hundred kilo hertz. The major characteristics of these transformer is fixed the voltage levels of source in the secondary side and primary side, provides the isolation between the input source and load. dc-dc converters using high frequency transformers have the following working modes: flyback, forward, push-pull, half bridge, full bridge.

1. Flyback and forward topology

Forward topology is based on buck function, while flyback topology is based on boost function. As shown in Fig. 2-1, isolate forward dc-dc converter topology is shown. Isolate forward dc-dc converter topology includes one switch, one transformer, one inductor, one capacitor, two diodes, and resistance load.

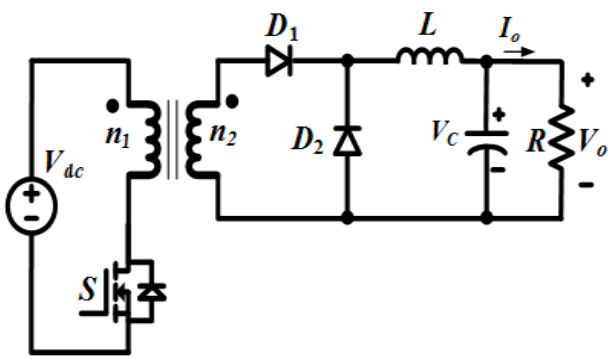

Fig. 2-1 Isolate forward dc-dc converter topology

In this mode, relation between output voltage and input voltage can be given by:

$$\frac{V_0}{V_{dc}} = \frac{n_2}{n_1} D \tag{2.1}$$

where D represents duty ratio.

As shown in Fig. 2-2, Isolate flyback dc-dc converter topology is shown. Isolate flyback dc-dc converter topology includes one switch, one inductor, one transformer, one capacitor, one diode, and resistance load.

In this mode, relation between output voltage and input voltage can be given by:

$$\frac{V_0}{V_{dc}} = \frac{n_2}{n_1} \frac{D}{1-D} \tag{2.2}$$

This is the type of power source transmitted indirectly through the transformer. The output voltage can be higher or less than the input voltage. From a single input source can give multiple output voltages. The flyback power supply allows for multiple output voltages. While other types of power supplies are not as reliable or accurate.

2. Push-pull topology

Fig. 2-3 shows isolate push-pull dc-dc converter topology. Isolate push-pull dc-dc converter topology includes two switches, one transformer, one inductor, one capacitor, two diodes, and resistance load. Relation between output voltage and input voltage can be given by:

$$\frac{V_0}{V_{dc}} = \frac{n_2}{n_1} D \tag{2.3}$$

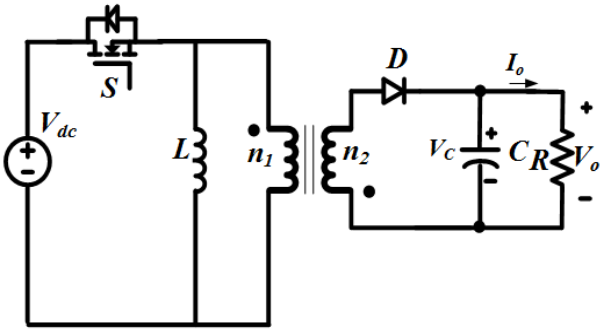

Fig. 2-2 Isolate flyback dc-dc converter topology

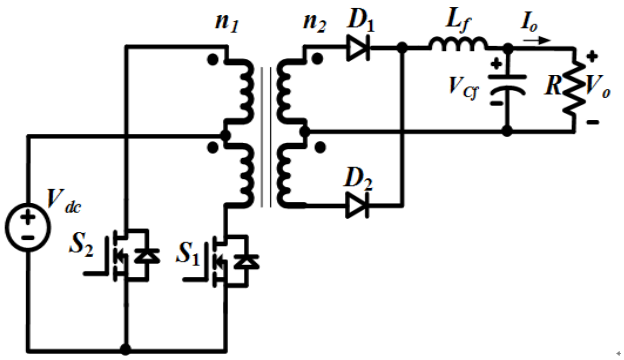

Fig. 2-3 Isolate push-pull dc-dc converter topology

This is a type of pulsed power source that is transmitted indirectly through a transformer. The output voltages can be less or higher than the input voltage. It is called pulling power source. By continuously switching two S_1 and S_2 switches, there is always a constant current on the load. Because of this advantage, the push-pull source for variable performance is the highest.

3. The conventional current-fed full bridge topology

In half bridge topology, relation between output voltage and input voltage can be given by:

$$\frac{V_0}{V_{dc}} = \frac{n_2}{2n_1} D \tag{2.4}$$

In full bridge topology relation between output voltage and input voltage can be given by:

$$\frac{V_0}{V_{dc}} = \frac{n_2}{2n_1} \frac{1}{1-D} \tag{2.5}$$

The current-fed topology produces a zero point at the primary side of the transformer when four switches are switched on.

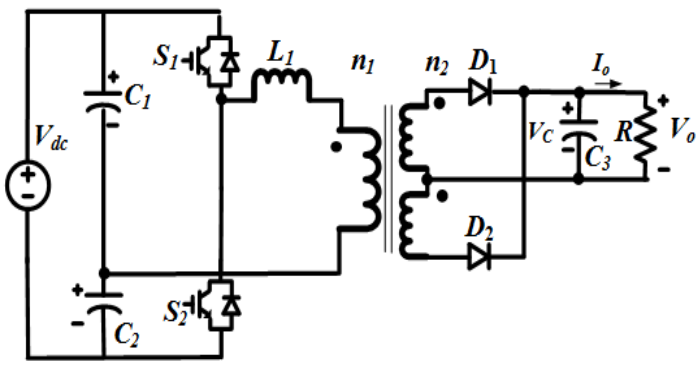

Fig. 2-4 Conventional current-fed half bridge isolated boost dc-dc converter

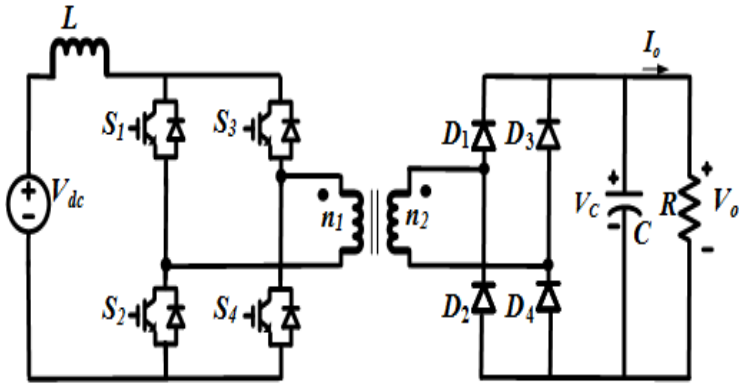

Fig. 2-5 Conventional current-fed full bridge isolated boost dc-dc converter

B. Non-isolation Configuration

The classic non-isolation dc-dc converters include buck, boost, and buck-boost topology. With different inductances, switches, and diodes, these converters perform different goals, but the principle of operation is based on the phenomenon of maintaining current through the inductance.

1. Boost dc-dc converter topology

Its main application is in regulated dc power supplies and the regenerative braking of dc motors. As the name implies, the output voltage is always greater than the input voltage. When the switch is on, the diode is reversed biased, thus isolating the output stage.

a. Continuous mode

In continuous mode, the current through the inductor is always higher than zero. Fig. 2-6 shows the typical waveforms of currents and equivalent circuit of the boost converter in continuous mode.

In on mode as shown in Fig. 2-6(a), switch S is switched on, the diode D is blocked and inductor L is charged.

In off mode as shown in Fig. 2-6(b), switch S is switched off, the diode D conducts. The inductor L is discharged. The energy released in the inductance causes the output voltage of the converter to always rise higher than the input voltage.

The output voltage can be expressed

$$V_{out} = \frac{1}{1-D} V_{dc} \tag{2.6}$$

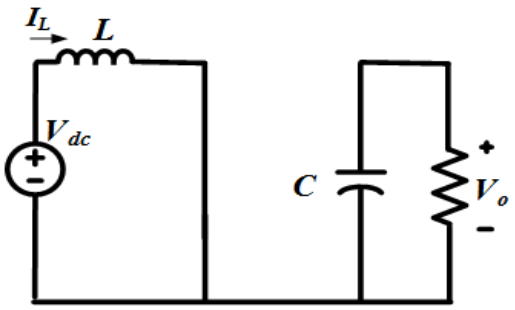

(a) On mode

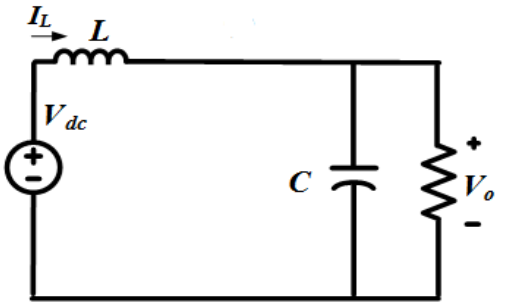

(b) Off mode

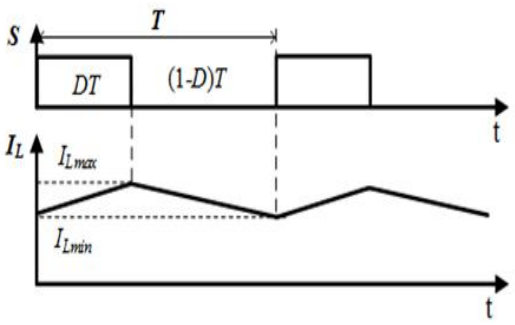

(c) Steady-state waveforms for the boost converter

Fig. 2-6 Equivalent circuit of the boost converter in continuous mode

b. Discontinuous mode

In discontinuous mode, the ripple value of the current through the inductor is too high. the current through the inductor drops to zero before the end of a whole switching cycle. Fig. 2-7 shows the typical waveforms of currents and equivalent circuit of the boost converter in discontinuous mode. The boost converter commonly operates in discontinuous mode under light loads.

In discontinuous mode, the current through the inductor drops to zero as shown in Fig. 2-7.

The output voltage gain In discontinuous mode can be written as follows:

$$\frac{V_{out}}{V_{dc}} = 1 + \frac{D^2 T V_{dc}}{2LI_0} \tag{2.7}$$

To understand the discontinuous-current-conduction mode, we would assume that as the output load power decreases, V_{dc} and D remain constant. Waveforms at the boundary of continuous conduction and discontinuous co assuming that V_{dc} and D are constant.

The discontinuous current conduction occurs due to decreased $P_0(=P_d)$ and, hence, a lower $I_L(=I_d)$, since V_d is constant. Since $I_{L,Peak}$ is the same in both modes, a lower value of I_L is possible only if V_0 goes up.

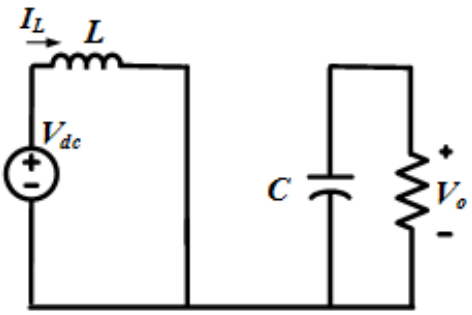

(a) On mode

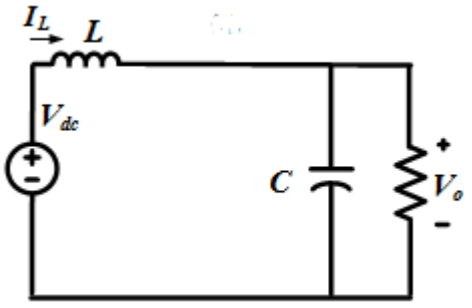

(b) Off mode

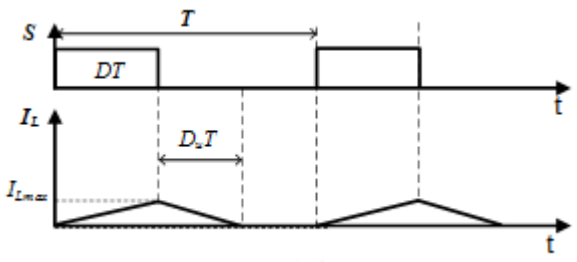

(c) Steady-state waveforms for the boost converter

Fig. 2-7 Equivalent circuit of the boost converter in discontinuous mode

2. Buck dc-dc converter topology

Fig. 2-8 and Fig. 2-9 present the buck converter topology and operation of the buck converter, respectively. The output voltage is given as follow:

$$V_o = D \cdot V_{dc} \tag{2.8}$$

As the name implies, a step-down converter produces a lower average output voltage than the dc input voltage V_{dc}. Its main application is in regulated dc power supplies and dc motor speed control.

Conceptually, the basic circuit constitutes a step-down converter for a purely resistive load. Assuming an ideal switch, a constant instantaneous input voltage V_{dc}, and a purely resistive load, the instantaneous output voltage waveform is a function of the switch position. The average output voltage can be calculated in therms of the switch duty ratio.

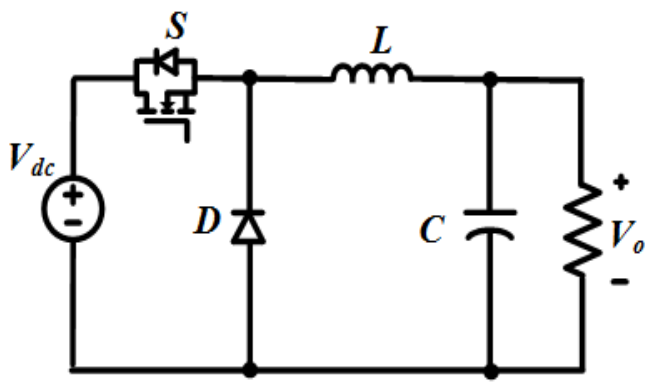

Fig. 2-8 Buck converter topology

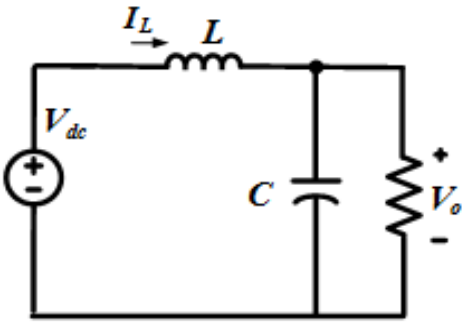

(a) On mode

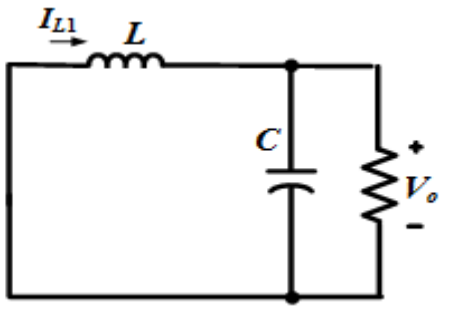

(b) Off mode

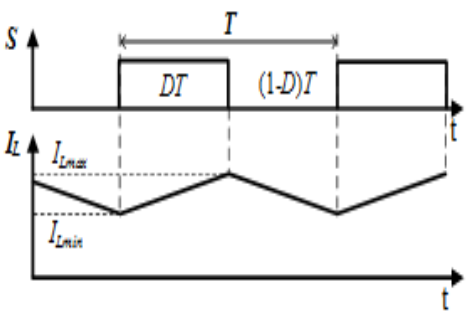

(c) Steady-state waveforms for the buck converter

Fig. 2-9 Equivalent circuit of the buck converter

3. Buck-boost dc-dc converter topology

The circuit as shown in Fig. 2-10 is a buck-boost converter because the output voltage can be higher or less than the input voltage by adjusting the duty ratio D.

The output voltage is given as follow

$$\frac{V_o}{V_{dc}} = \frac{D}{1-D} \tag{2.9}$$

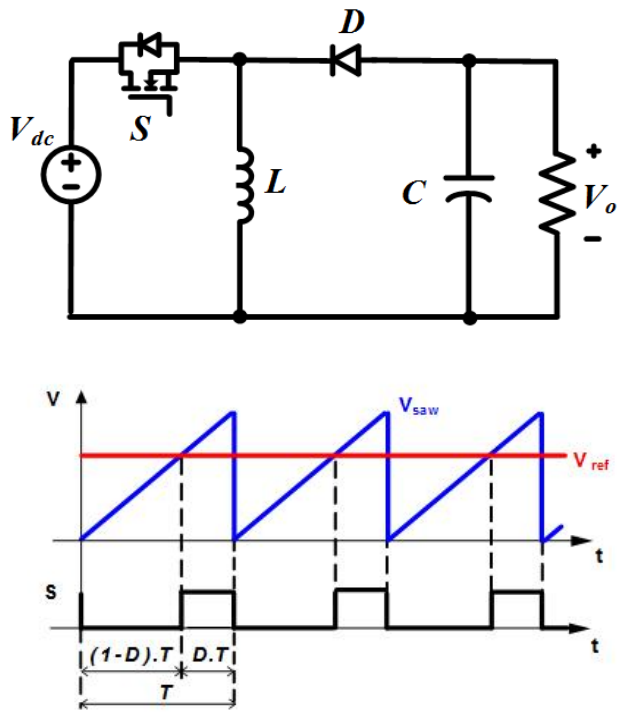

Fig. 2-10 Buck-boost converter topology

4. Interleaved boost converter topology

Similar to basic boost dc-dc converter topology, the interleaved boost converter topology [27] as shown in Fig. 2-11 also converts a low input voltage to a higher output voltage. Besides that, the interleaved boost converter topology have some additional merits such as high efficiency and low ripple input current. When switch S_a is switched on and switch S_b is switched off. The diode D_1 is blocked while the diode D_2 conducts since the input voltage is less than the input voltage.

The inductor L_1 are charged while the inductor L_2 delivering energy to the load and the output capacitor. When switch S_b is switched on and switch S_a is switched off. The diode D_2 is blocked while the diode D_1 conducts since the input voltage is less than the input voltage.

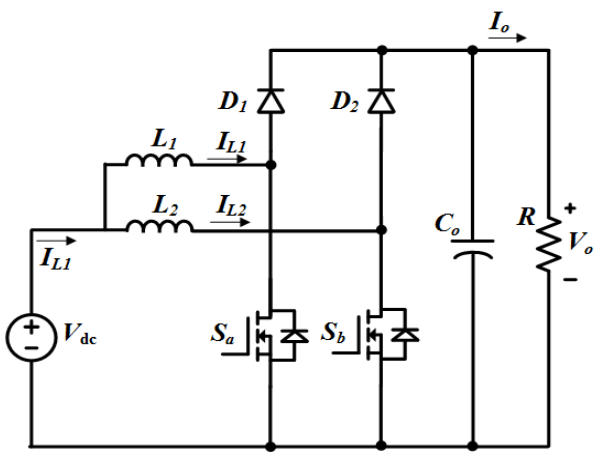

Fig. 2-11 Interleaved boost converter topology

The inductor L_2 are charged while the inductor L_1 delivering energy to the load and the output capacitor. When two switches S_a and S_b are switched off. Diode D_1 and diode D_2 conduct since the input voltage is less than the input voltage. The inductor L_2 and the inductor L_1 delivering energy to the load and the output capacitor.

The output voltage can be expressed:

$$V_{out} = \frac{1}{1-D} V_{in} \tag{2.10}$$

5. High step-up stacked dc-dc converter topology

Fig. 2-12 shows stacked dc-dc converter topology to get a high voltage gain with high efficiency [36]. In this converter topology have some merits such as a high step-up conversion ratio and low voltage stress across components. Due to low voltage stress across semiconductor devices, this converter topology allows the use of faster semiconductor devices with low voltage.

As a results, it can operate at higher switching frequency than traditional topologies, since the reduced switch voltage stress. The output voltage gain of this converter topology is given by:

$$V_o = V_{dc} \cdot (1 + \frac{1}{1-D} + \frac{D}{(1-D)^2} + \frac{D^2}{(1-D)^3}) \tag{2.11}$$

The switch voltage stress in all switches are given by:

$$\begin{cases} V_{s1} = V_{dc}\dfrac{1}{1-D} \\ V_{s2} = V_{dc}\dfrac{D}{(1-D)^2} \\ V_{s3} = V_{dc}\dfrac{D^2}{(1-D)^3} \end{cases} \tag{2.12}$$

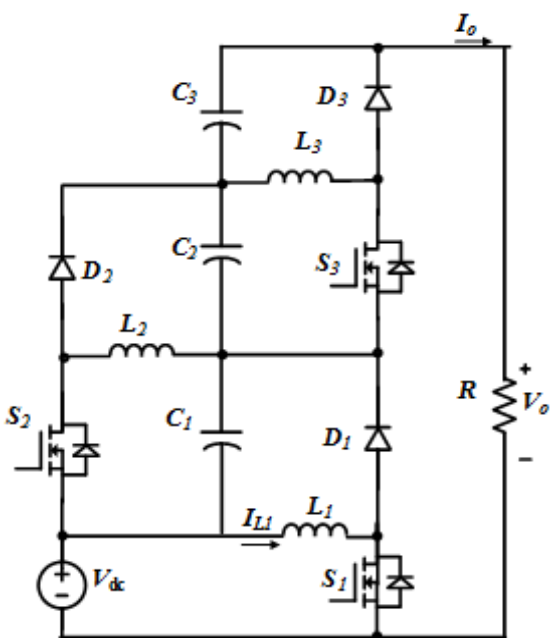

Fig. 2-12 Stacked dc-dc converter topology

Ⅲ. Proposed High gain DC-DC Boost type Converter

A. Proposed topology

1. Circuit analysis in continuous conduction mode

Fig. 3-1 illustrates the proposed high gain dc-dc boost type converter. The proposed converter consists of two inductors (L_1 and L_2), two active-switches(S_a and S_b), a boost capacitor(C_1), six diodes, one input voltage source and a capacitor(C_o) directly connecting with a resistive load(R) in parallel. The two active-switches are controlled by two signal with a different phase of 180 degrees. From Fig. 3-4, It is easy to see that the operating frequency of two inductors is double of switching frequency of the switches. As a result, size of the inductors is dropped. The proposed high gain dc-dc boost type converter has three operating states in continuous conduction mode(CCM) as shown in Fig. 3-2. To simplify the circuit analysis, the components in proposed converter were assumed to be ideal.

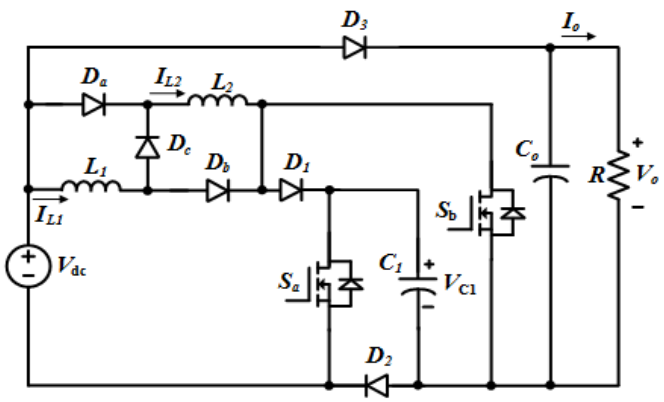

Fig. 3-1 Proposed Converter

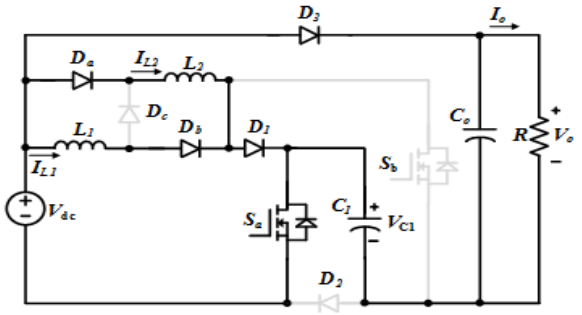

(a) State 1

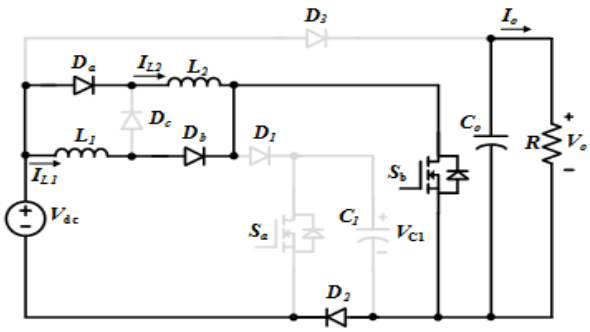

(b) State 2

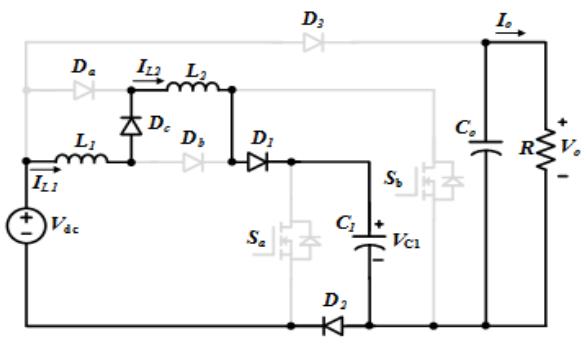

(c) State 3

Fig. 3-2 Operating states of the proposed converter in continuous conduction mode

In the state 1 as shown in Fig. 3-2(a), the switch S_a is switched on while the switch S_b is switched off. The diodes, D_C and D_2 are blocked while the diodes, D_a, D_b, D_1 and D_3 are conducting. Capacitor C_1 is discharged while two inductors (L_1 and L_2) and capacitor C_o are charged. The time interval in this mode is D·T, where T and D are the switching period and the duty cycle of S_a, respectively. With $i_i * i_s$ the input dc current during state 1 when Switch S_a is switched on. We have

$$\begin{cases} L_1 = \dfrac{di_{L1}}{dt} = L_2 \dfrac{di_{L2}}{dt} = V_{dc} \\ V_o = V_{c1} + V_{dc} \\ C_1 \dfrac{d\nu_{c1}}{dt} = I_{L1} + I_{L2} - i_{i*} \\ C_o \dfrac{d\nu_{co}}{dt} = i_{in} - I_{L1} - I_{L2} - I_o \end{cases} \tag{3.1}$$

In the state 2 as shown in Fig. 3-2(b), the switch S_b is switched on while the switch S_a is switched off. The diodes, D_1, D_3 and D_C are blocked while the diodes, D_a, D_b and D_3 are conducting. Capacitor C_o is discharged while two inductors, L_1 and L_2 are charged. The time interval in this mode is D·T. We have

$$\begin{cases} L_1 \dfrac{di_{L1}}{dt} = L_2 \dfrac{di_{L2}}{dt} = V_{dc} \\ C_1 \dfrac{d\nu_{c1}}{dt} = 0 \\ C_o \dfrac{d\nu_{co}}{dt} = - I_o \end{cases} \tag{3.2}$$

In the state 3 as shown in Fig. 3-2 (c), the switches S_a and S_b are switched off. The diodes, D_1, D_2 and D_C are conducting while the diodes, D_a,

D_b and D_3 are blocked. Capacitor C_1 is charged while two inductors (L_1 and L_2) and capacitor C_o are discharged. The time interval in this mode is (1-2D)·T, where T and D are the switching period and the duty cycle of S_a, respectively. We have

$$\begin{cases} L_1\dfrac{di_{L1}}{dt}+L_2\dfrac{di_{L2}}{dt}=V_{dc}-V_{c1} \\ C_1\dfrac{d\nu_{c1}}{dt}=I_{L1}=I_{L2} \\ C_o\dfrac{d\nu_{co}}{dt}=-I_o \end{cases} \tag{3.3}$$

Using the volt-second balance law to the inductor, from (3.1), (3.2) and (3.3), we have

$$\begin{cases} V_{c1}=\dfrac{1+2D}{1-2D}V_{dc} \\ I_{L1}=I_{L2}=\dfrac{1}{1-2D}I_o \end{cases} \tag{3.4}$$

From (3.1) and (3.4), the output voltage, V_o of the proposed converter in discontinuous conduction mode is

$$V_o=V_{dc}+V_{C1}=\frac{2}{1-2D}V_{dc} \tag{3.5}$$

2. Circuit analysis in discontinuous conduction mode

When light loads are used, the proposed high gain dc-dc boost type converter will operate in the in discontinuous conduction mode. This operating mode causes an over boost effect in the output and capacitor voltages. Fig. 3-4 (b) shows the typical waveforms of the proposed high gain dc-dc boost

type converter in the DCM

In the state 1 as shown in Fig. 3-3 (a), the switch S_a is switched on while the switch S_b is switched off. The diodes, D_C and D_2 are blocked while the diodes, D_a, D_b, D_1 and D_3 are conducting. Capacitor C_1 is discharged while two inductors (L_1 and L_2) and capacitor C_o are charged. The time interval in this mode is D·T. With $i_i * i_s$ the input dc current during state 1 when switch S_a is switched on. We have

$$\begin{cases} L_1 = \dfrac{di_{L1}}{dt} = L_2 \dfrac{di_{L2}}{dt} = V_{dc} \\ V_o = V_{c1} + V_{dc} \\ C_1 \dfrac{d\nu_{c1}}{dt} = I_{L1} + I_{L2} - i_{i*} \\ C_o \dfrac{d\nu_{co}}{dt} = i_{in} - I_{L1} - I_{L2} - I_o \end{cases} \tag{3.6}$$

In the state 2 as shown in Fig. 3-3(b), the switches S_a and S_b are switched off. The diodes, D_1, D_2 and D_C are conducting while the diodes, D_a, D_b and D_3 are blocked. Capacitor C_1 is charged while two inductors (L_1 and L_2) and capacitor C_o are discharged. The time interval in this mode is D_u·T. We have

$$\begin{cases} L_1 \dfrac{di_{L1}}{dt} + L_2 \dfrac{di_{L2}}{dt} = V_{dc} - V_{c1} \\ C_1 \dfrac{d\nu_{c1}}{dt} = I_{L1} = I_{L2} \\ C_o \dfrac{d\nu_{co}}{dt} = - I_o \end{cases} \tag{3.7}$$

In the state 3 as shown in Fig. 3-3 (c), the switch S_b is switched on while the switch S_a is switched off. The diodes, D_1, D_3 and D_C are blocked while

the diodes, D_a, D_b and D_3 are conducting. Capacitor C_o is discharged while two inductors, L_1 and L_2 are charged. The time interval in this mode is D·T. We have

$$\begin{cases} L_1 \dfrac{di_{L1}}{dt} = L_2 \dfrac{di_{L2}}{dt} = V_{dc} \\ C_1 \dfrac{d\nu_{c1}}{dt} = 0 \\ C_o \dfrac{d\nu_{co}}{dt} = -I_o \end{cases} \tag{3.8}$$

In the state 4 as shown in Fig. 3-3 (d), the switches S_a and S_b are switched off. We have

$$C_o \frac{d\nu_{Co}}{dt} = -I_o \tag{3.9}$$

From Fig. 3-4 (b), the average inductor L_1 current is calculated as

$$\overline{I_{L1}} = \triangle I_{L1}(D+D_u)T = \frac{V_{dc}}{L_1} D(D+D_u)T \tag{3.10}$$

Using the volt-second balance theory to the inductor in the DCM in a steady state, we obtain;

$$D_u = \frac{4D \cdot V_{dc}}{V_{c1} - V_{dc}} \tag{3.11}$$

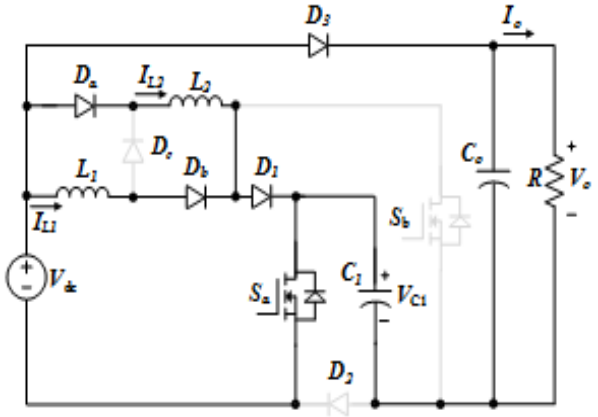

(a) State 1

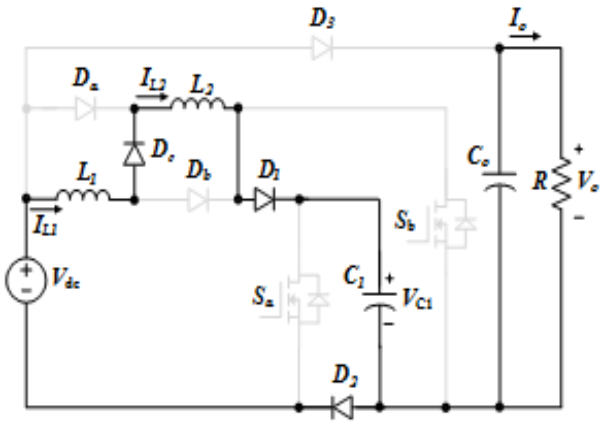

(b) State 2

Fig. 3-3 Operating states of the proposed converter in discontinuous conduction mode

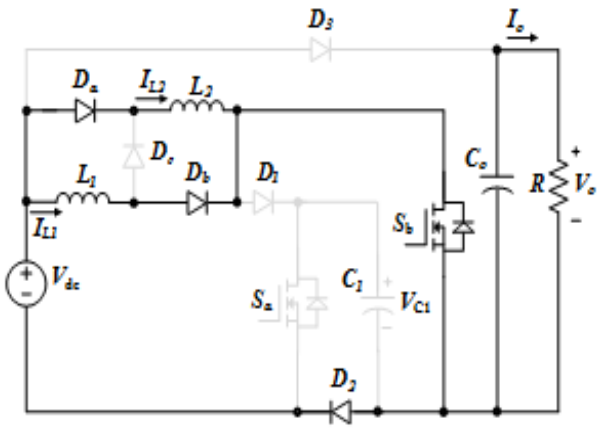

(c) State 3

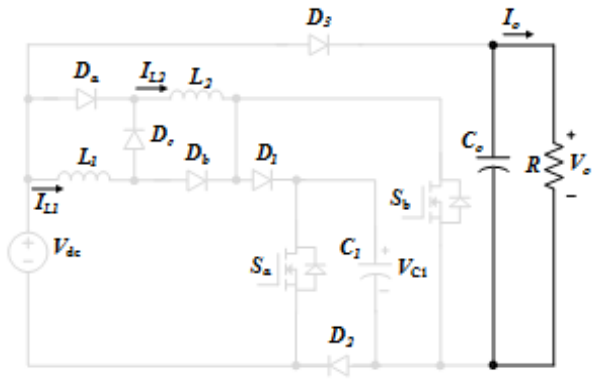

(d) State 4

Fig. 3-3 (continued from the previous page)

B. Proposed PWM control strategy

Fig. 3-4 shows the PWM strategy of the proposed high gain dc-dc boost type converter. A high-frequency carrier waveform, V_{tri} is compared to the reference voltage, V_{SH} to produce the control signals of S_b switch. The other reference voltage ($1-V_{SH}$) is used to compare to the high-frequency carrier waveform, V_{tri} to produce the control signals of S_a switch.

In the PWM switching at a constant switching frequency, the switch control signal, which controls the state (on or off) of the switch, is generated by comparing a signal-level control voltage $v_{control}$ with a repetitive waveform. The control voltage signal generally is obtained by amplifying the error, or the difference between the actual output voltage and its desired value. The frequency of the repetitive waveform with a constant peak, which is shown to be a sawtooth, establishes the switching frequency. This frequency is kept constant in a PWM control and is chosen to be in a few kilohertz to a few hundred kilohertz rage. When the amplified error signal, which varies very slowly with time relative to the switching frequency, is greater than the sawtooth waveform, the switch control signal becomes high, causing the switch to turn on. Otherwise, the switch is off. In terms of $v_{control}$ and the peak of the sawtooth wave form V_{st}.

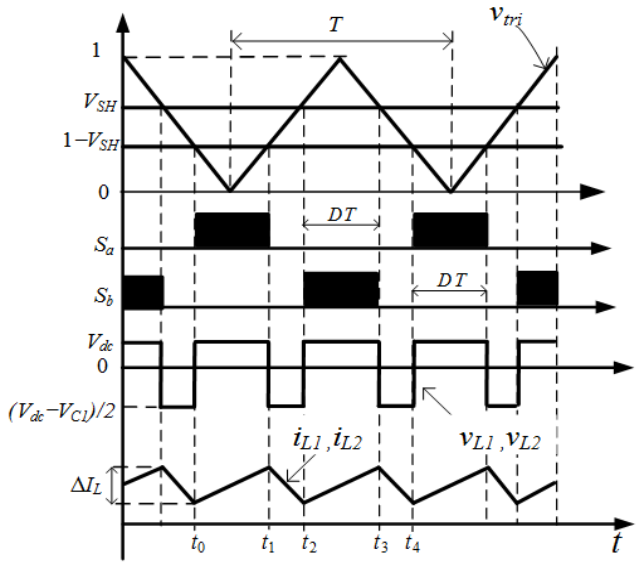

(a) CCM mode

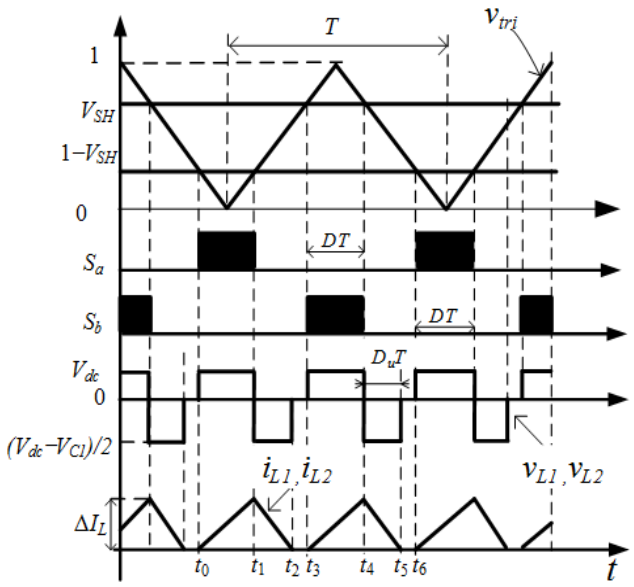

(b) DCM mode

Fig. 3-4 The phase shift PWM control strategy of the proposed high gain dc-dc boost type converter

Ⅳ. Extend Proposed High Gain DC-DC Boost Type Converter

A. High gain dc-dc boost type converter using 2-switched-inductor cell

Fig. 4-1 presents the proposed high gain dc-dc boost type converter using 2-switched-inductor cells. Compared to the proposed high gain dc-dc boost type converter using 2-switched-inductor cells as shown in the chapter 3, the proposed high gain dc-dc boost type converter using 2-switched-inductor cells uses more 1-switched-inductor cell. As shown in Fig. 4-1, the proposed topology using 2-switched-inductor cells consists of two active-switches(S_a and S_b), three inductors(L_1, L_2, and L_3), nine diodes, a boost capacitor(C_1), one input voltage source and a capacitor(C_o) directly connecting in parallel with a resistive load(R) in parallel.

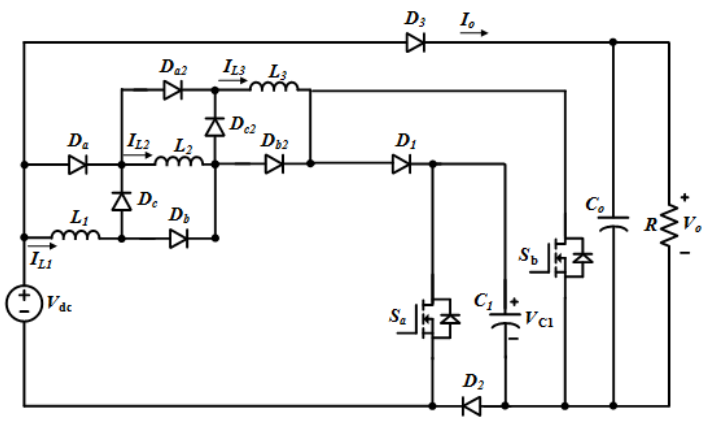

Fig. 4-1 Proposed high gain dc-dc boost type converter using 2-switched-inductor cell

Similar to the high gain dc-dc boost type converter topology, the proposed topology using 2 switched-inductor cells also has three operating states in CCM as shown in Fig. 4-2. In the state 1, three inductors and capacitor(C_o) are charged while capacitor(C_1) is discharged as shown in Fig. 4-2 (a). We have:

$$\begin{cases} L_1\dfrac{di_{L1}}{dt}=L_2\dfrac{di_{L2}}{dt}=L_3\dfrac{di_{L3}}{dt}=V_{dc} \\ V_o=V_{C1}+V_{dc} \\ C_1\dfrac{d\nu_{C1}}{dt}=I_{L1}+I_{L2}+I_{L3}-i_{in*} \\ C_o\dfrac{d\nu_{Co}}{dt}=i_{\in *}-I_{L1}-I_{L2}-I_{L3}-I_o \end{cases} \tag{4.1}$$

Where i_{in*} is the input dc current during state 1 when switch S_a is switched on.

In the state 2, Capacitor C_o is discharged while three inductors are charged as shown in Fig. 4-2 (b). Capacitor C_1 is disconnected from the main circuit. We have:

$$\begin{cases} L_1\dfrac{di_{L1}}{dt}+L_2\dfrac{di_{L2}}{dt}+L_3\dfrac{di_{L3}}{dt}=V_{dc}-V_{C1} \\ C_1\dfrac{d\nu_{C1}}{dt}=I_{L1}=I_{L2}=I_{L3} \\ C_o\dfrac{d\nu_{Co}}{dt}=-I_o \end{cases} \tag{4.2}$$

In the state 3, the capacitor C_1 is charged while three inductors and capacitor C_o are discharged as shown in Fig. 4-2 (c). We have:

$$\left\{\begin{array}{l} L_1\frac{di_{L1}}{dt}=L_2\frac{di_{L2}}{dt}=L_3\frac{di_{L3}}{dt}=V_{dc} \\ C_1\frac{d\nu_{C1}}{dt}=0 \\ C_o\frac{d\nu_{Co}}{dt}=-I_o \end{array}\right\} \quad (4.3)$$

From (4.1), (4.2) and (4.3), we have

$$\left\{\begin{array}{l} V_{c1}=\frac{1+4D}{1-2D}V_{dc} \\ I_{L1}=I_{L2}=\frac{1}{1-2D}I_o \end{array}\right\} \quad (4.4)$$

The output voltage, V_o of the proposed converter topology using 2 switched-inductor cells is

$$V_o=V_{dc}+V_{C1}=\frac{2+2D}{1-2D}V_{dc} \quad (4.5)$$

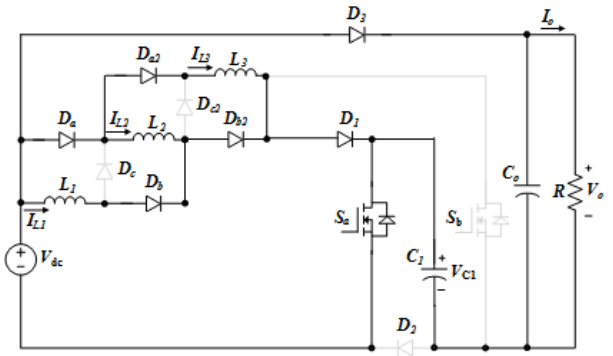

(a) State 1

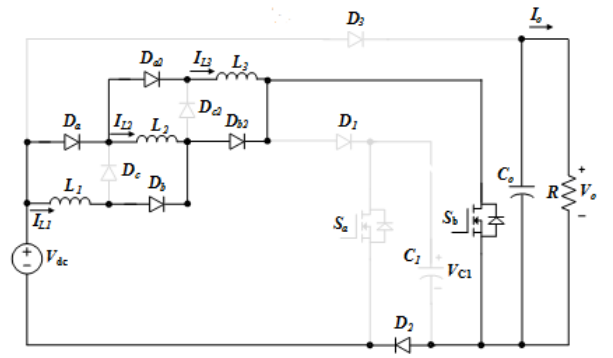

(b) State 2

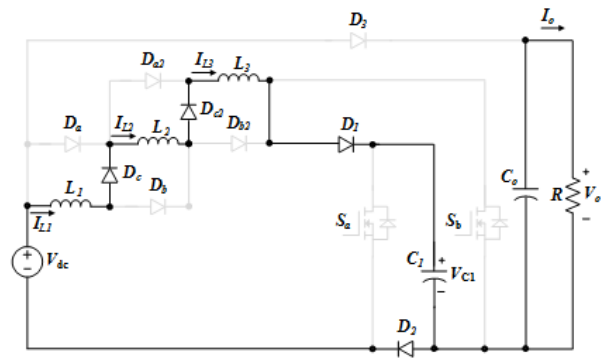

(c) State 3

Fig. 4-2 Operating states of the proposed converter using 2-switched-inductor cells

B. Extend proposed high gain dc-dc boost type converter

The structure of a switched-inductor cell consists of one inductor and three diodes as indicated in Fig. 4-3. In order to achieve larger boost ability, the proposed converter topology can be extended by adding more switched-inductor cells into the main circuit. The structure of a switched-inductor cell is shown in Fig. 4-4.

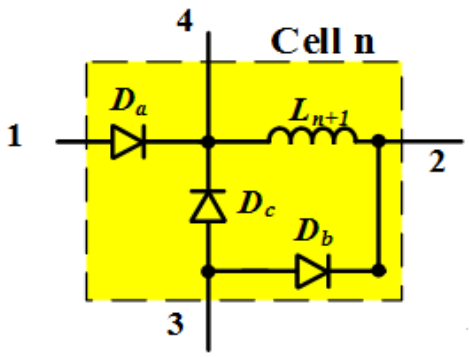

Fig. 4-3 The structure of a switched-inductor cell

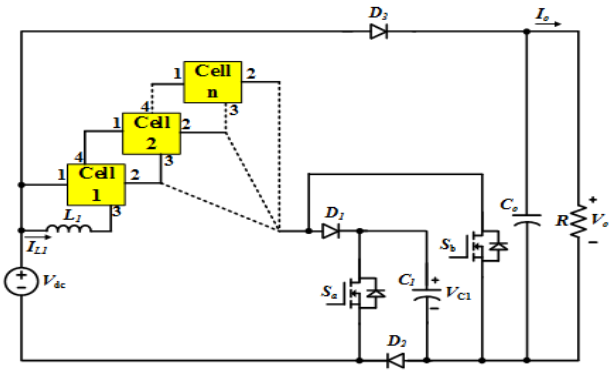

Fig. 4-4 Proposed converter using multi-cell switched-inductor

The proposed high gain dc-dc boost type converter using n-switched-inductor cells is shown in Fig. 4-4.

The capacitor(C_1) voltage of the proposed converter topology using n-switched-inductor cells can be derived as

$$V_{C1} = \frac{1+2nD}{1-2D} V_{dc} \tag{4.6}$$

The output voltage, V_o of the proposed converter topology using n-switched-inductor cells is

$$V_o = \frac{2+2(n-1)D}{1-2D} V_{dc} \tag{4.7}$$

The voltage gain, G of the proposed converter topology using n-switched-inductor cells is

$$G = \frac{V_o}{V_{dc}} = \frac{2+2(n-1)D}{1-2D} \tag{4.8}$$

Fig. 4-5 illustrates voltage gain comparison with using n-switched-inductor cells. As shown in Fig. 4-5, for the same duty cycle, D, increasing the number of cell rises voltage gain.

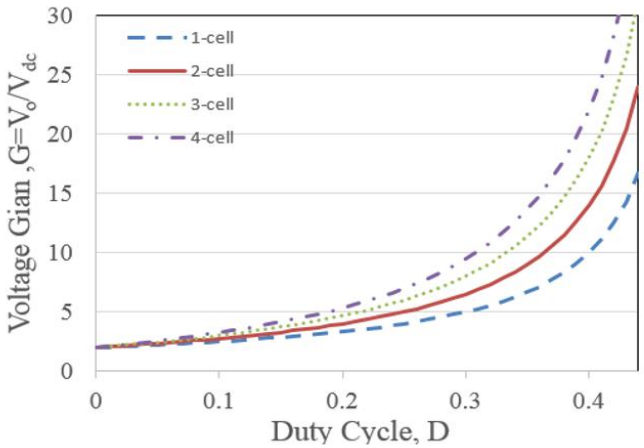

Fig. 4-5 Resultant comparative plots of voltage gain and duty cycle with using n-switched-inductor cells

C. Guidelines for passive components design of proposed converter

The two inductors L_1 and L_2 in the proposed converter are designed based on the peak-to-peak current ripple. The peak-to-peak ripple of the inductors current as shown in Fig. 3-4 is defined as

$$\triangle I_{L1} = \triangle I_{L2} = \frac{V_{dc}}{L_1} DT \tag{4.9}$$

From (4.9), the inductors, L_1 and L_2 are calculated as

$$L_1 = L_2 = \frac{2DTV_{gdc}^2}{x\%P_o} \tag{4.10}$$

where x% is the ripple ratio of the inductor L_1 current and is defined as $x\%=\triangle I_{L1}/I_{L1}$.

The peak value of inductor currents can be given by

$$I_{L1\_p} = I_{L2\_p} = \frac{(1+0.5 \cdot x\%)}{2V_g} P_o \tag{4.11}$$

The capacitor C_1 is also selected according to the capacitor C_1 voltage ripple. As shown in Fig. 3-2 (c), the peak-peak ripple value of capacitor C_1 voltage is defined as

$$\triangle V_{c1} = \frac{(0.5-D)T \cdot I_{L1}}{C_1} \tag{4.12}$$

From (4.12), the capacitor C_1 is calculated as

$$C_1 = \frac{(0.5-D)^2 TP_o}{(1+2D)\, V_g^2 \cdot y\%} \tag{4.13}$$

where y% are the ripple ratio of the capacitor C_1 voltage and is defined as y% = $\triangle V_{C1}/V_{C1}$ and P_o is output power. The voltage stress on the capacitor C_1 defined as (3.4).

Similarly, the capacitor C_o are also selected according to the capacitor C_o voltage ripple. As shown in Fig. 3-2(b) and Fig. 3-2 (c), the peak-peak ripple value of capacitor C_o voltage is defined as

$$\triangle V_o = \frac{I_o(1-D)\,T}{C_o} \tag{4.14}$$

From (4.14), the capacitor C_o is calculated as

$$C_o = \frac{(1-D)(1-2D)^2 P_o T}{4V_g^2 \cdot z\%} \tag{4.15}$$

where z% are the ripple ratio of the capacitor C_o voltage and is defined as z%=$\triangle V_{C1}/V_{C1}$.

The voltage stress on the capacitor C_o is the same as the output voltage V_o.

Ⅴ. Simulation and Experimental Results

A. Simulation results

In this section, the simulation results on PSIM simulation is shown to confirm the accuracy of calculated equations, indicated analyses and operating characteristics for the proposed high gain dc-dc boost type converter. The configurations of the proposed inverter are as follow: L_1=L_2=700 μH, C_1=68 μF, C_o=220 μF, and R=200 Ω.The switching frequency is 20 kHz. An output DC voltage of 400 V can be produced from a low input voltage. Table 5-1 illustrates a list of the parameters of the proposed high gain dc-dc boost type converter parameters used in the simulation.

Table 5-1 Parameters for simulation

Parameter		Value
Input voltage (V_{dc})		25 V - 100 V
Output voltage (V_o)		400 V
Output power		800 W
Inductors	L_1	700 μH
	L_2	700 μH
Capacitor	C_1	68 μF
	C_0	220 μF
Resistor load		200 Ω
Switching frequency		20 kHz

1. Simulation results of proposed converter using 1-switched-inductor cells

a. Simulation results with voltage gain, G=8

Similarly, in order to provide voltage gain of 8, the value of duty cycle, D is fixed at 0.375. Fig. 5-1 ~ Fig. 5-6 show the simulation results of the proposed high gain dc-dc boost type converter with G = 8. As shown in Fig. 5-1, the voltage of the C_1 is boosted to 350 V from the low input voltage of 50 V. The output voltage and output current are 399.7 V and 2 A, respectively. Diode D_a voltage waveform, diode D_b voltage waveform, and diode D_c voltage waveform are the square waveformas shown in Fig. 5-2. The maximum voltage across the diode D_a and diode D_b are 150 V meanwhile that of diode D_c is 50 V. The maximum voltage across the diode D_3 is 350 V.

Similarly, in order to provide voltage gain of 8, the value of duty cycle, D is fixed at 0.375. Fig. 5-1 ~ Fig. 5-6 show the simulation results of the proposed high gain dc-dc boost type converter with G=8.

As shown in Fig. 5-1, we can see that the voltage of the C_1 is boosted to 350 V from the low input voltage of 50 V. The output voltage and out put current are 399.7 V and 2 A, respectively. Diode D_a voltage waveform, diode D_b voltage waveform, and diode D_c voltage waveform are the square waveform as shown in Fig. 5-2. The maximum voltage across the diode D_a and diode D_b are 150 V meanwhile that of diode D_c is 50 V.

(a) Input voltage (V_{dc})

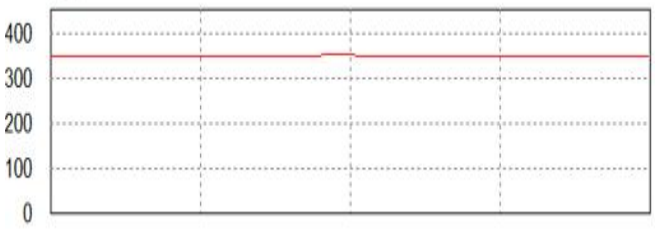

(b) C_1 capacitor voltage (V_{c1})

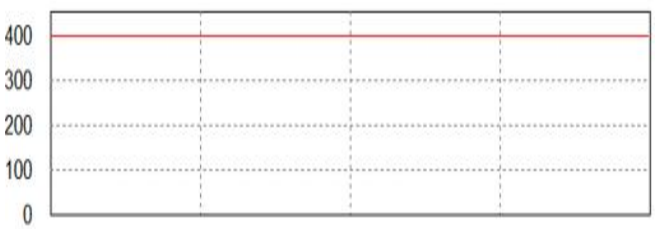

(c) Output voltage (V_o)

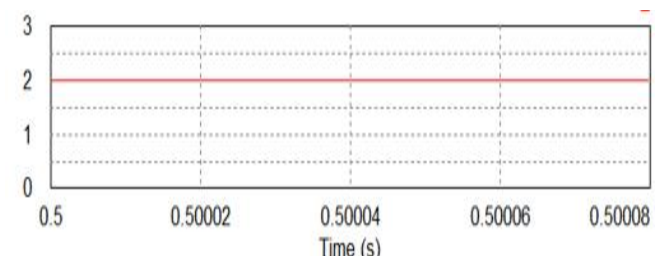

(d) Load current (I_o)

Fig. 5-1 Simulation waveforms of the proposed converter when V_{dc}= 50 V

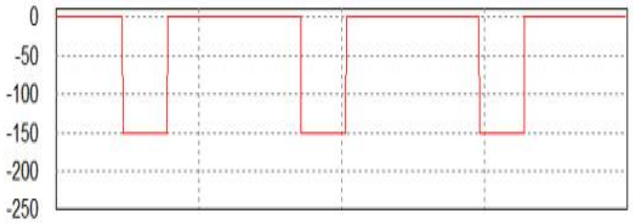

(a) Diode S_a voltage (V_{Da})

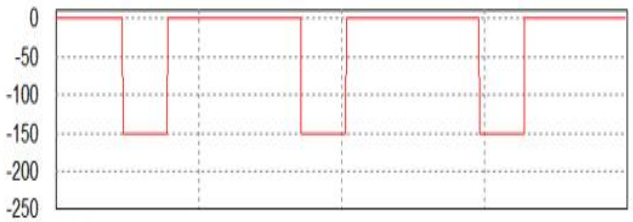

(b) Diode D_b voltage (V_{Db})

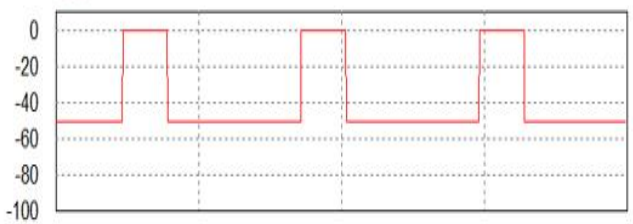

(c) Diode D_c voltage (V_{Dc})

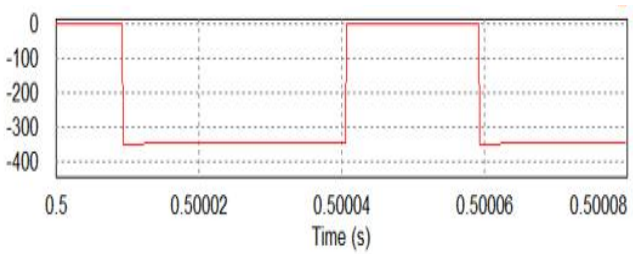

(d) Diode D_3 voltage (V_{D3})

Fig. 5-2 Simulation waveforms of the proposed converter when V_{dc}= 50 V

The maximum voltage across the diode D_3 is 350 V From Fig. 5-3, we can see that diode D_1 voltage, diode D_2 voltage, switch S_a voltage and switch S_b voltage also are the square waveform and are 349.9 V.

The voltage across on inductor L_1 and L_2 are the same value. The voltage across on inductor L_1 and L_2 equal to -150 V in the state 3 and 50 V in the state 1 and 2. The inductor L_1 current and inductor L_2 current are the same value and are 8 A. As shown in Fig. 5-4, the current ripple on inductor L_1 and inductor L_2 are 1 A.

Fig. 5-5 shows the current waveform on diodes D_a, D_b and D_c. The current stress on diodes D_a, D_b and D_c is equal to the inductor current and are 8 A. Fig. 5-6 shows the current waveform on D_1 diode, D_2 diode, S_a switch and S_b switch. The current stress on diodes D_1 and D_2 is 17 A and the current stress on switches S_a and S_b also is 17 A.

(a) Switch S_a voltage (V_{ds-sa})

(b) Switch S_b voltage (V_{ds-sb})

(c) Diode D_1 voltage (V_{D1})

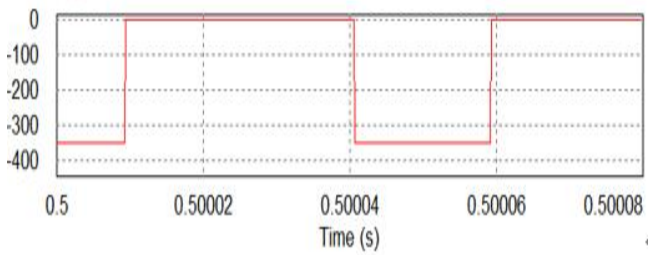

(d) Diode D_2 voltage (V_{D2})

Fig. 5-3 Simulation waveforms of the proposed converter when V_{dc}= 50 V

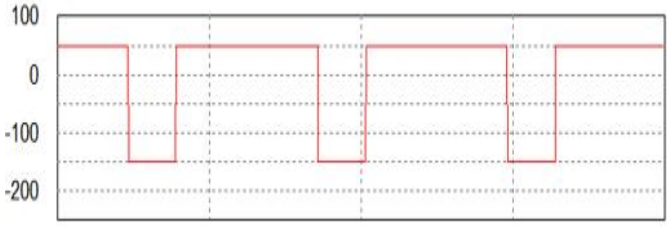

(a) Voltage across inductor L_1 (V_{L1})

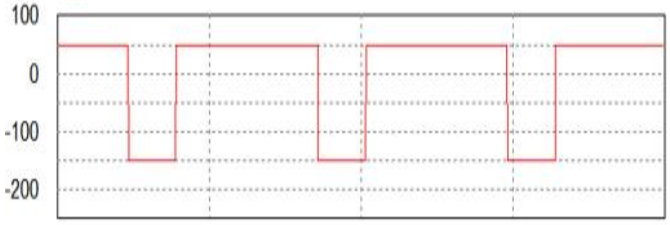

(b) Voltage across inductor L_2 (V_{L2})

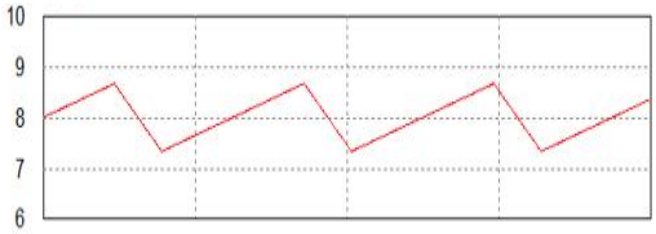

(c) Inductor L_1 current (i_{L1})

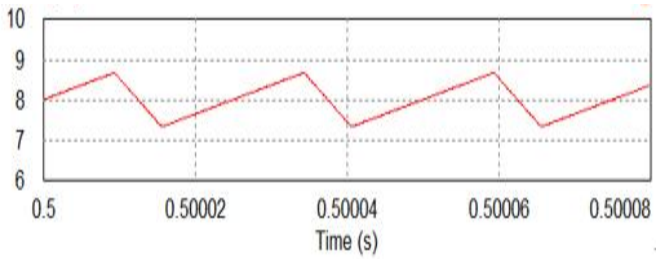

(d) Inductor L_2 current (i_{L2})

Fig. 5-4 Simulation waveforms of the proposed converter when V_{dc}= 50 V

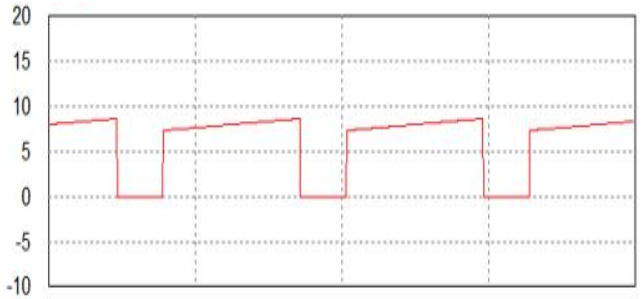

(a) Diode D_a current (i_{Da})

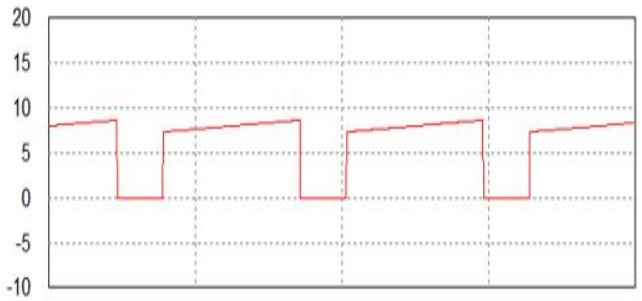

(b) Diode D_b current (i_{Db})

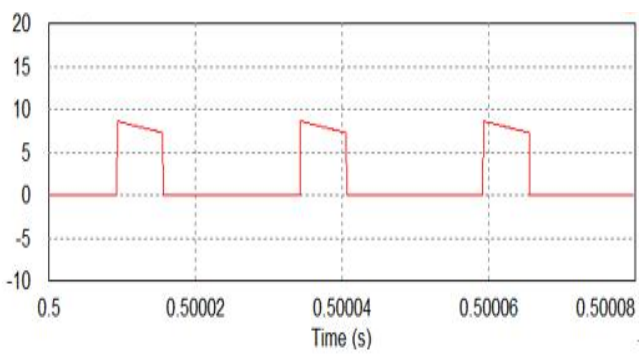

(c) Diode D_c current (i_{Dc})

Fig. 5-5 Simulation waveforms of the proposed converter when V_{dc}= 50 V

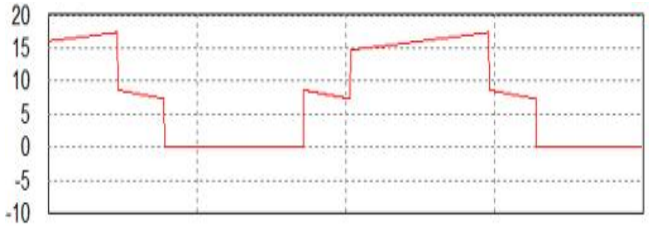

(a) Diode D_1 current(i_{D1})

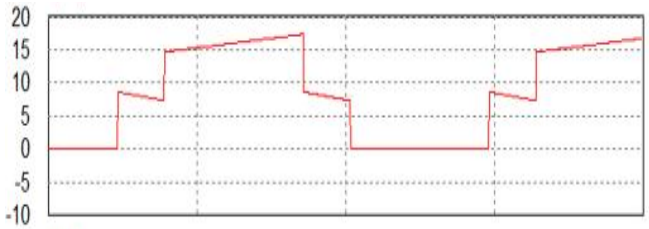

(b) Diode D_2 current(i_{D2})

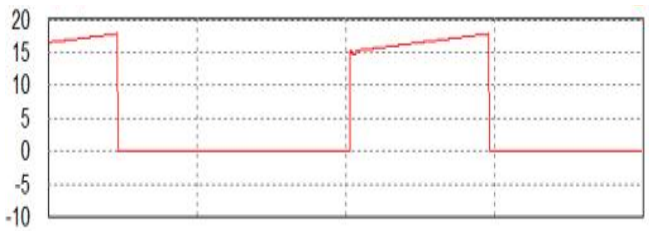

(c) Switch S_a current (i_{Sa})

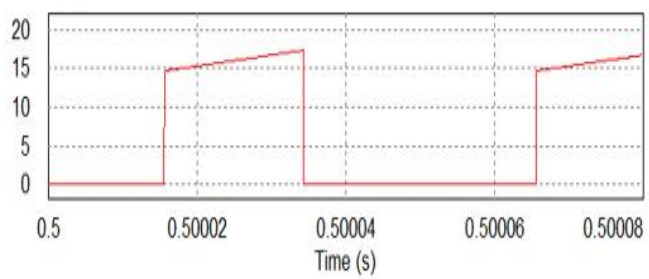

(d) Switch S_b current (i_{Sb})

Fig. 5-6 Simulation waveforms of the proposed converter when V_{dc} = 50 V

Table 5-2 shows a comparison between the calculation results and simulation results of the proposed high gain dc-dc boost type converter with G=8. As shown in Table 5-2, the value in simulation results is less than those in the calculation results because the ripple current on the inductor and ripple voltage ripple on capacitor are ignored in the calculation results.

Table 5-2 Voltage and current stresses with G=8

		Calculation value	Simulation value
Output voltage (V_o)		400 V	399.7 V
Capacitors voltage	C_1	350 V	350 V
	C_o	400 V	399.7 V
Output power	D_1	350 V	349.9 V
	D_2	350 V	349.9 V
	D_3	350 V	349.6 V
	D_a	150 V	150 V
	D_b	150 V	150 V
	D_c	50 V	50 V
Switches voltage	S_a	350 V	349.9 V
	S_b	350 V	349.9 V
Inductor current	L_1	8 A	8 A
	L_2	8 A	8 A

b. Simulation results with voltage gain, G=4

To provide voltage gain of 4, the value of duty cycle, D is fixed at 0.25. Fig. 5-7 ~ Fig. 5-12 show the simulation results of the proposed high gain dc-dc boost type converter with G=4.

As shown in Fig. 5-7, the voltage of the C_1 is boosted to 300 V from the low input voltage of 100 V. The output voltage and output current are 399.1 V and 2 A, respectively.

Diode D_a voltage waveform, diode D_b voltage waveform, and diode D_c voltage waveform are the square waveform as shown in Fig 5-8. The maximum voltage across the diode D_b and diode D_c are 100 V meanwhile that of diode D_c is 99.9 V. The maximum voltage across the diode D_3 is 299.1 V.

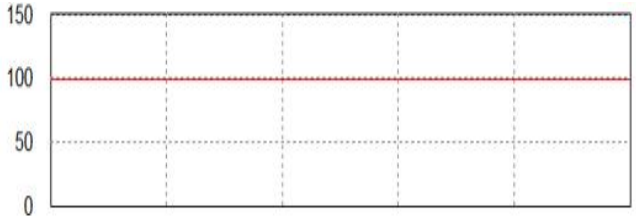

(a) Input voltage (V_{dc})

(b) C1 capacitor voltage (V_{c1})

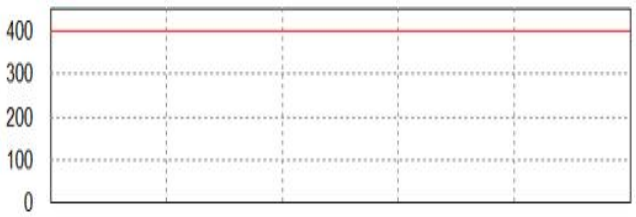

(c) Output voltage (V_o)

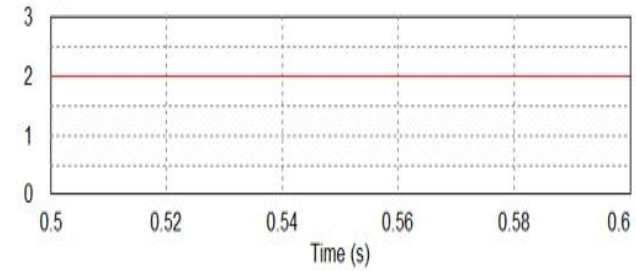

(d) Load current (I_o)

Fig. 5-7 Simulation waveforms of the proposed converter when V_{dc}= 100 V

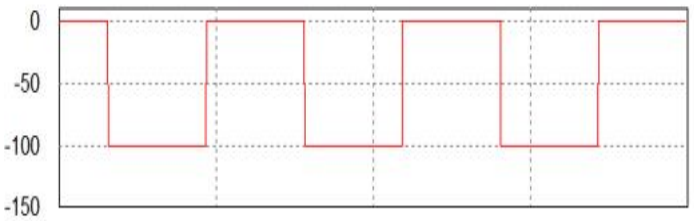

(a) Diode D_a voltage (V_{Da})

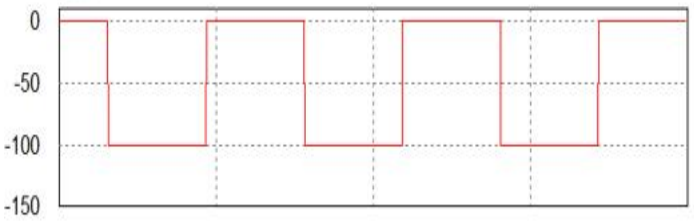

(b) Diode D_b voltage (V_{Db})

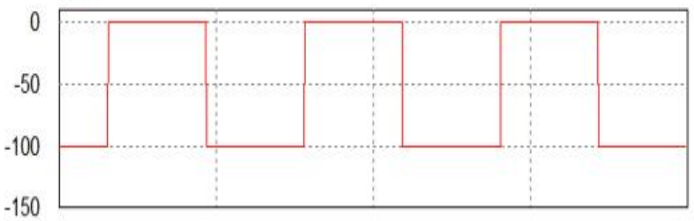

(c) Diode D_c voltage (V_{Dc})

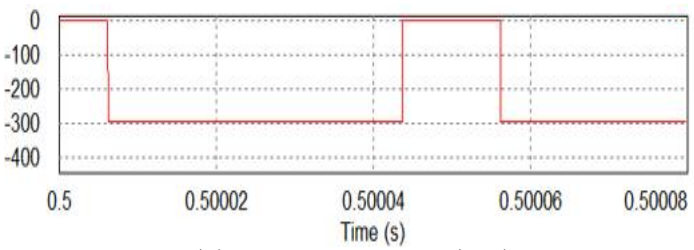

(d) Diode D_3 voltage (V_{D3})

Fig. 5-8 Simulation waveforms of the proposed converter when V_{dc}= 100 V

(a) Switch S_a voltage (V_{ds-sa})

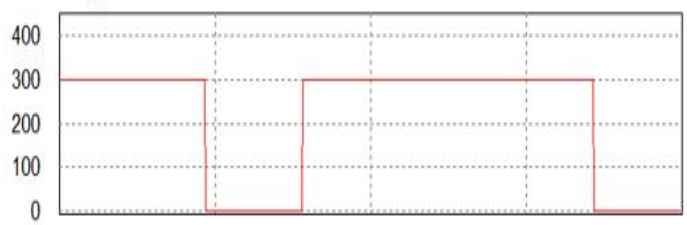

(b) Switch S_b voltage (V_{ds-sb})

(c) Diode D_1 voltage (V_{D1})

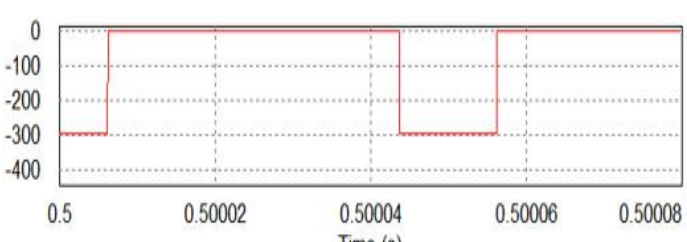

(d) Diode D_2 voltage (V_{D2})

Fig. 5-9 Simulation waveforms of the proposed converter when V_{dc}= 100 V

From Fig. 5-9, we can see that diode D_1 voltage, diode D_2 voltage, switch S_a voltage and switch S_b voltage also are the square waveform and are 300 V. The voltage across on inductor L_1 and L_2 are the same value. The voltage across on inductor L_1 and L_2 equal to -100 V in the state 3 and 100 V in the state 1 and 2. The inductor L_1 current and inductor L_2 current are the same value and are 4 A. As shown in Fig. 5-10, the current ripple on inductor L_1 and inductor L_2 are 1.75 A.

Fig. 5-11 shows the current waveform on diodes D_a, D_b and D_c. The current stress on diodes D_a, D_b and D_c is equal to the inductor current and are 4 A.

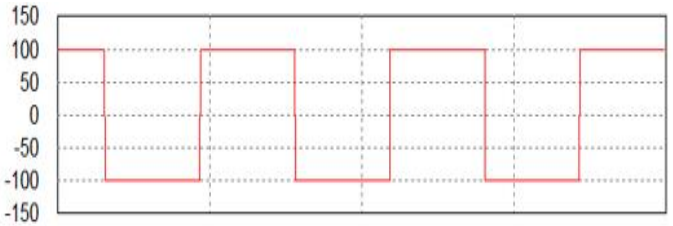

(a) Voltage across inductor L_1 (V_{L1})

(b) Voltage across inductor L_2 (V_{L2})

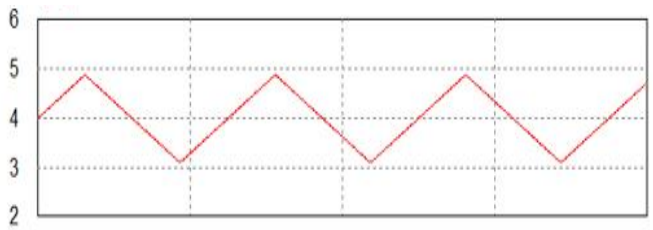

(c) Inductor L_1 current (i_{L1})

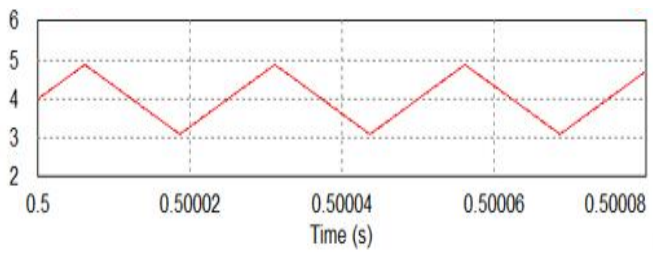

(d) Inductor L_2 current (i_{L2})

Fig. 5-10 Simulation waveforms of the proposed converter when V_{dc}= 100 V

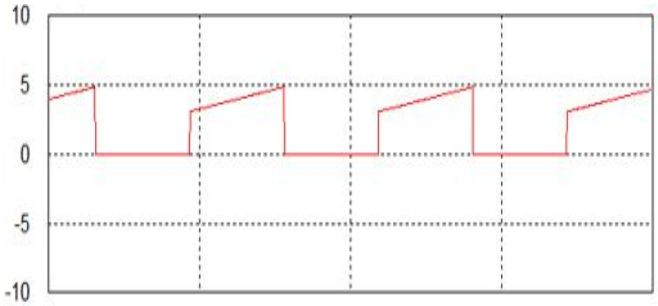

(a) Diode D_a current (i_{Da})

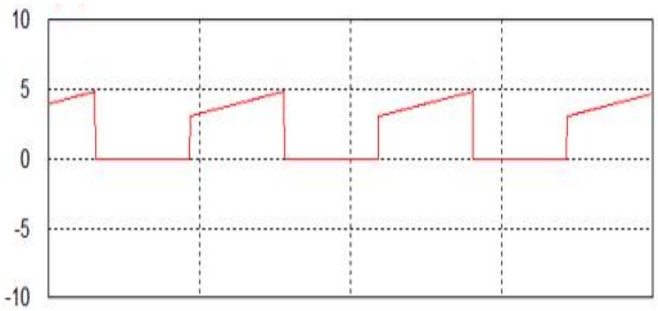

(b) Diode D_b current (i_{Db})

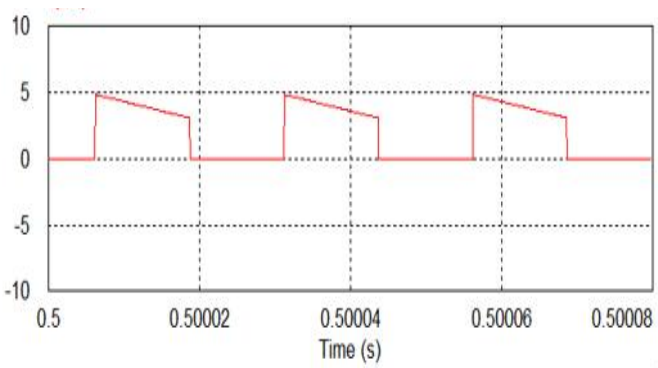

(c) Diode D_c current (i_{Dc})

Fig. 5-11 Simulation waveforms of the proposed converter when V_{dc}= 100 V

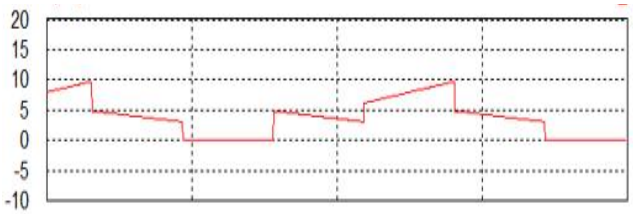

(a) Diode D_1 current(i_{D1})

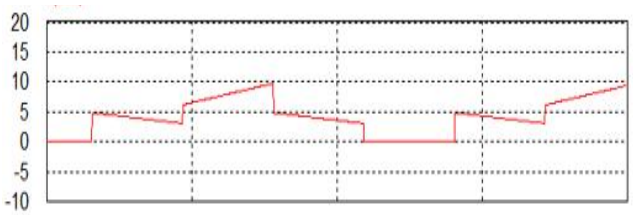

(b) Diode D_2 current(i_{D2})

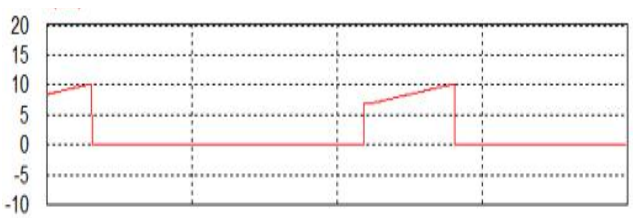

(c) Switch S_a current (i_{Sa})

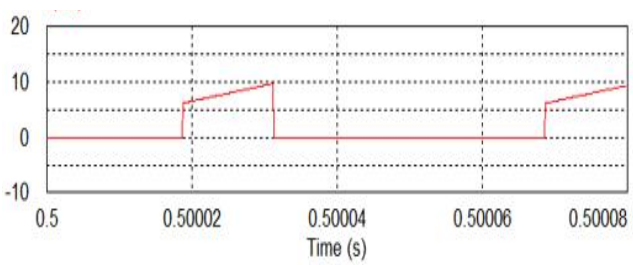

(d) Switch S_b current (i_{Sb})

Fig. 5-12 Simulation waveforms of the proposed converter when V_{dc}= 100 V

Fig 5-12 shows the current waveform on D_1 diode, D_2 diode, S_a switch and S_b switch. The current stress on diodes D_1 *and* D_2 is 10 A and the current stress on switches S_a and S_b also is 10 A.

Table 5-3 shows a comparison between the calculation results and simulation results of the proposed high gain dc-dc boost type converter with G=4. As shown in Table 5-3, the value in simulation results is less than those in the calculation results because the ripple current on the inductor and ripple voltage ripple on capacitor are ignored in the calculation results.

Table 5-3 Voltage and current stresses with G=4

		Calculation value	Simulation value
Output voltage (V_o)		400 V	399.1 V
Capacitors voltage	C_1	300 V	300 V
	C_o	400 V	399 V
Output power	D_1	300 V	300 V
	D_2	350 V	300 V
	D_3	350 V	299.1 V
	D_a	350 V	99.9 V
	D_b	100 V	100 V
	D_c	100 V	100 V
Switches voltage	S_a	300 V	300 V
	S_b	300 V	300 V
Inductor current	L_1	4 A	4 A
	L_2	4 A	4 A

2. Simulation results of proposed converter using 2-switched-inductor cells

The value of duty cycle, D is fixed at 0.412 to provide voltage gain of 16. Fig. 5-13 ~ Fig. 5-17 show the simulation results of the proposed high gain dc-dc boost type converter with G=16. As shown in Fig. 5-13, the voltage of the C_1 is boosted to 375 V from the low input voltage of 25 V. The output voltage and output current are 400 V and 2 A, respectively. Diode D_a voltage waveform, diode D_b voltage waveform, and diode D_c voltage waveform are the square waveform as shown in Fig. 5-14. The maximum voltage across the diode D_{a2} and diode D_{b2} are 116.7 V meanwhile that of diode D_{c2} is 25 V.

From Fig. 5-15, we can see that diode D_1 voltage, diode D_2 voltage, switch S_a voltage and switch S_b voltage also are the square waveform and are 374.5 V.

From Fig. 5-16, we can see that The voltage across on inductor L_1 and L_2 are the same value. The voltage across on inductor L_1 and L_2 equal to -116.7 V in the state 3 and 25 V in the state 1 and 2.

From Fig. 5-17, the inductor L_1 current inductor L_2 current and inductor L_3 current are the same value and are 11.38 A.

(a) Input voltage (V_{dc})

(b) C_1 capacitor voltage (V_{c1})

(c) Output voltage (V_o)

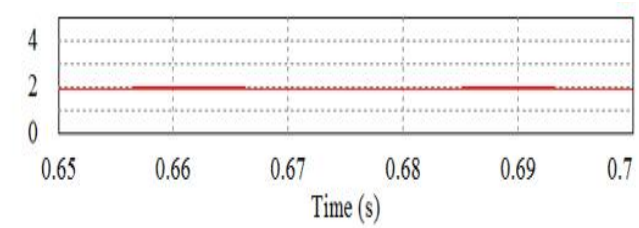

(d) Load current (I_o)

Fig. 5-13 Simulation waveforms of the proposed converter using *2*-switched-inductor cells when V_{dc}= 25 V

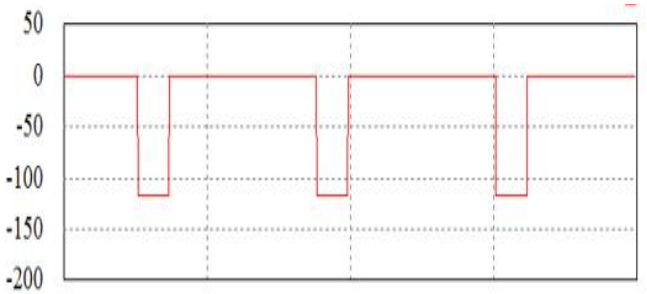

(a) Diode D_a voltage (V_{Da})

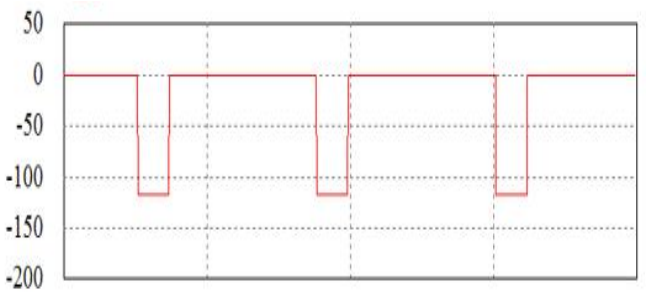

(b) Diode D_b voltage (V_{Db})

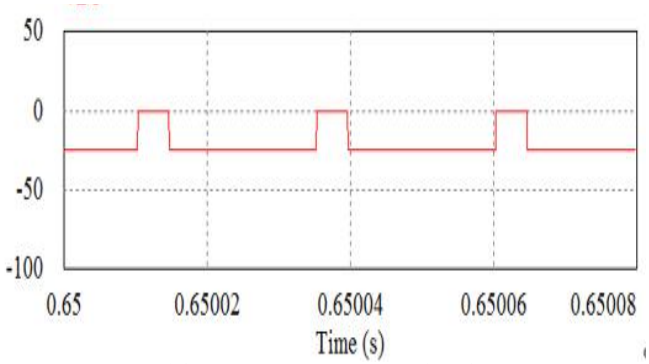

(c) Diode D_c voltage (V_{Dc})

Fig. 5-14 Simulation waveforms of the proposed converter using 2-switched-inductor cells when V_{dc}= 25 V

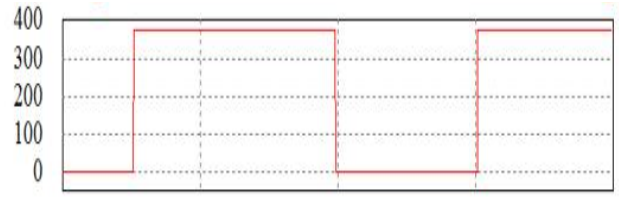

(a) Switch S_a voltage (V_{ds-sa})

(b) Switch S_b voltage (V_{ds-sb})

(c) Diode D_1 voltage (V_{D1})

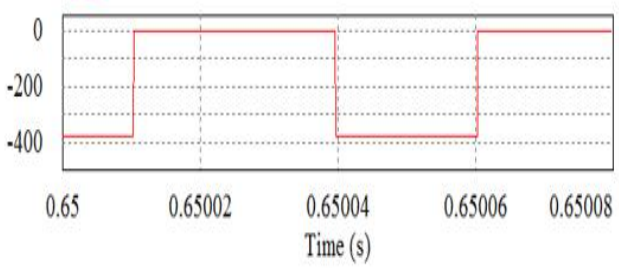

(d) Diode D_2 voltage (V_{D2})

Fig. 5-15 Simulation waveforms of the proposed converter using *2*-switched-inductor cells when V_{dc}= 25 V

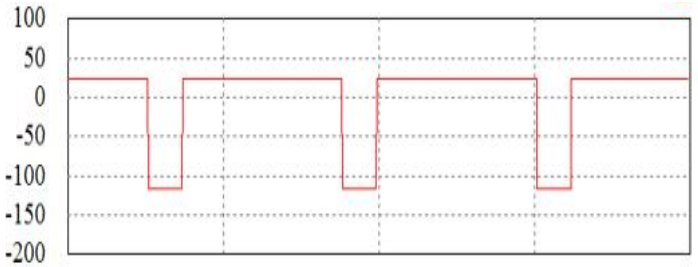

(a) Voltage across inductor L_1 (V_{L2})

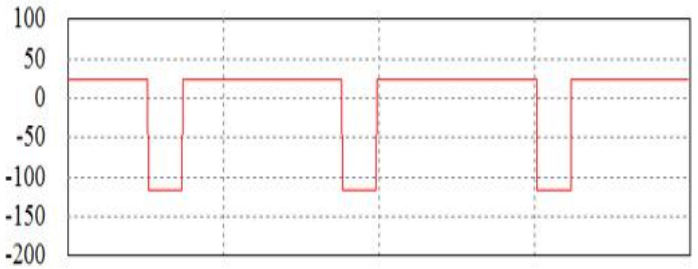

(b) Voltage across inductor L_2 (V_{L2})

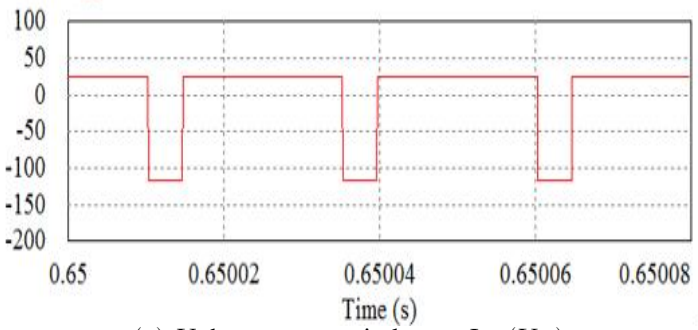

(c) Voltage across inductor L_3 (V_{L3})

Fig. 5-16 Simulation waveforms of the proposed converter using *2*-switched-inductor cells when V_{dc} = 25 V

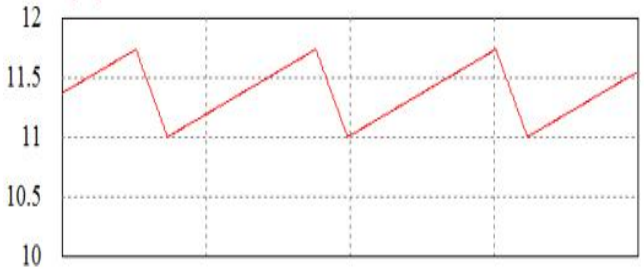

(a) Inductor L_1 current (i_{L1})

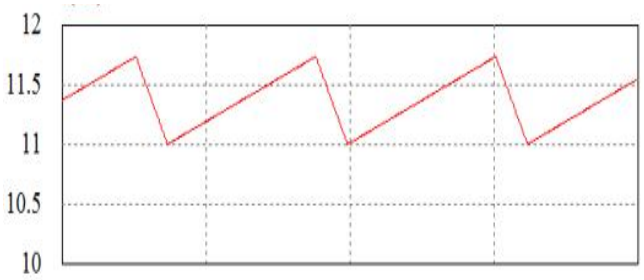

(b) Inductor L_2 current (i_{L2})

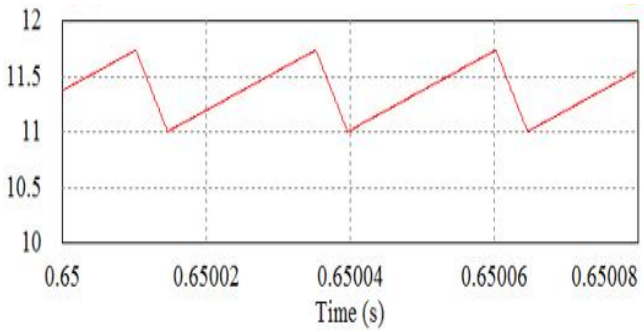

(c) Inductor L_3 current(i_{L3})

Fig. 5-17 Simulation waveforms of the proposed converter using 2-switched-inductor cells when V_{dc}= 25 V

3. Dynamic performance of proposed converter

The dynamic performance of proposed converter is shown in Fig. 5-18 ~ Fig. 5-21. In the first state, R=200 and input voltage changes from 50 V to 100 V. For this case, the simulation results by using PSIM software is shown in Fig. 5-18. According to Fig. 5-18, the output voltage reaches from 200 V to 400 V and the transient time is approximately 0.07 sec. In the second state, R = 200 and input voltage changes from 100 V to 50 V. The dynamic performance of proposed converter in the second state is shown in Fig. 5-19. According to Fig. 5-19, the output voltage drops from 400 V to 200 V and the transient time is approximately 0.047 sec. In the third state, V_{dc}=100 and output power changes from 400 W to 800 W.

The dynamic performance of proposed converter in the second state is shown in Fig. 5-20. In the last state, V_{dc} = 100 and output power changes from 800 W to 400 W. The dynamic performance of proposed converter in the second state is shown in Fig. 5-21.

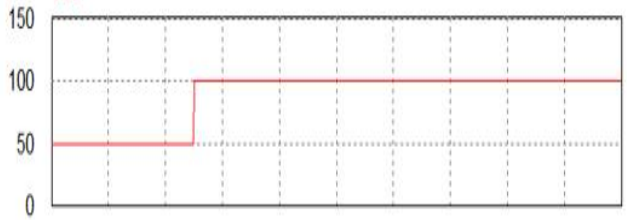

(a) Input voltage (V_{dc})

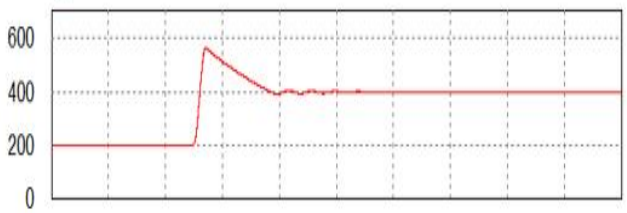

(b) Output voltage (V_o)

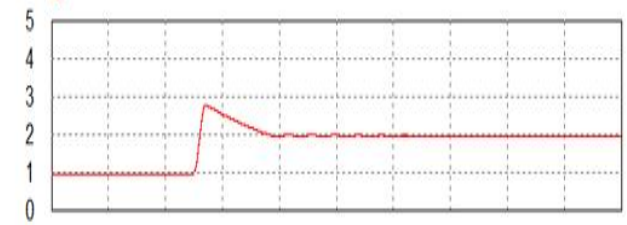

(c) Load current (I_o)

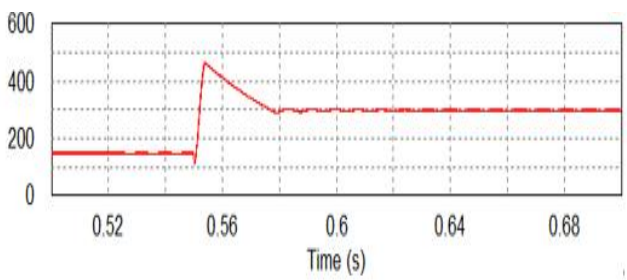

(d) C_1 capacitor voltage (V_{c1})

Fig. 5-18 Simulation waveforms of the proposed converter when input voltage changes from 50 V to 100 V

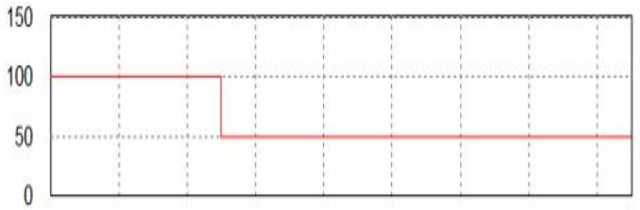

(a) Input voltage (V_{dc})

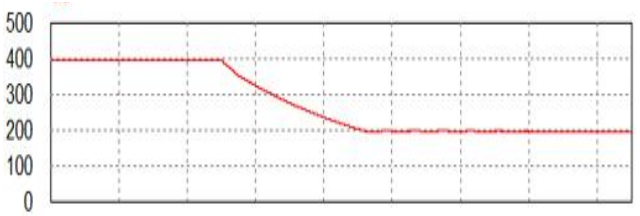

(b) Output voltage (V_o)

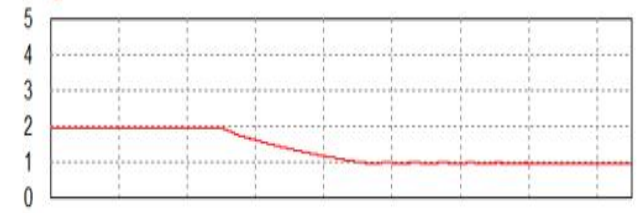

(c) Load current (I_o)

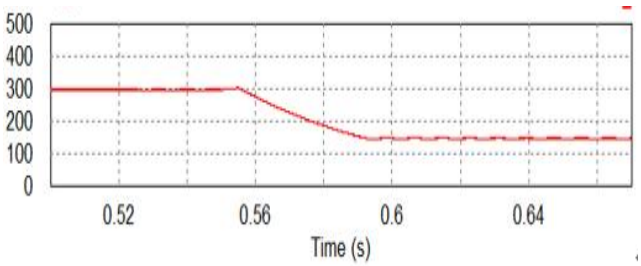

(d) C_1 capacitor voltage (V_{c1})

Fig. 5-19 Simulation waveforms of the proposed converter when input voltage changes from 100 V to 50 V

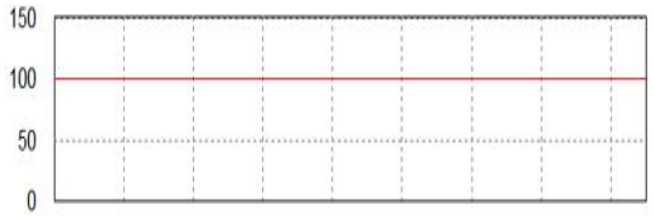

(a) Input voltage (V_{dc})

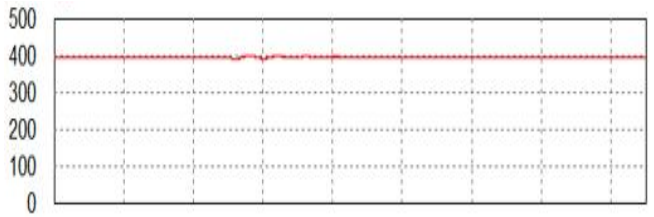

(b) Output voltage (V_o)

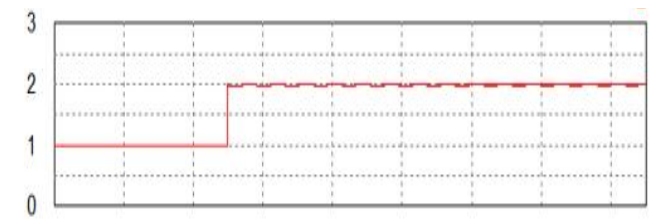

(c) Load current (I_o)

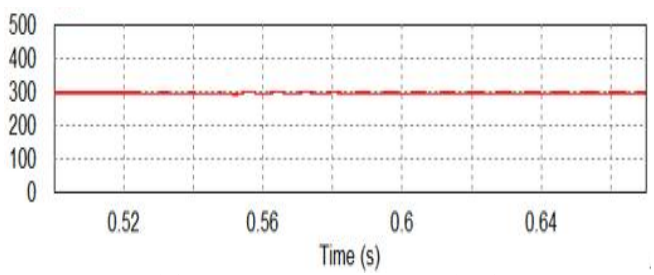

(d) C_1 capacitor voltage (V_{c1})

Fig. 5-20 Simulation waveforms of the proposed converter when output voltage changes from 400 W to 800 W

(a) Input voltage (V_{dc})

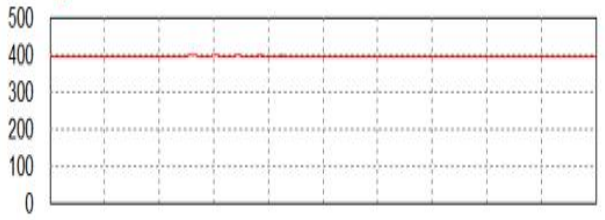

(b) Output voltage (V_o)

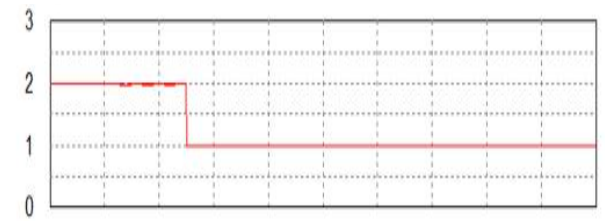

(c) Load current (I_o)

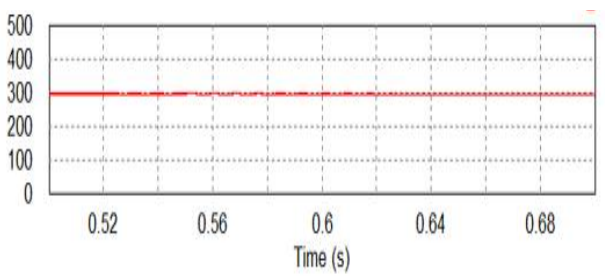

(d) C_1 capacitor voltage (V_{c1})

Fig. 5-21 Simulation waveforms of the proposed converter when output voltage changes from 800 W to 400 W

B. Experimental results

Based on the calculation and simulation results, the experiment prototype of the proposed high gain dc-dc boost type converter was developed as shown in Fig. 5-22. In this work, kit TMS320F28035 (i.e., clocked at frequency of 60 MHz) of Texas Instruments was used to implement the PWM scheme.

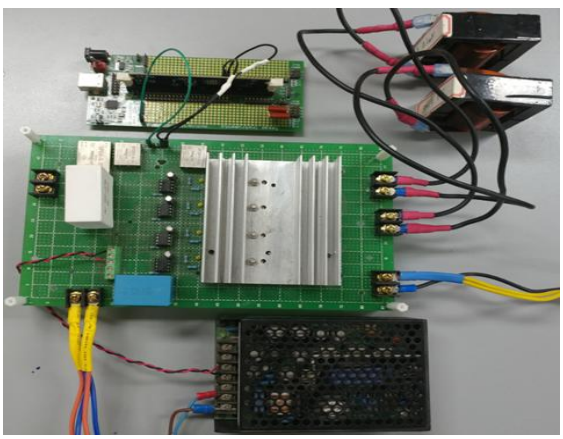

Fig. 5-22 Experimental setup of the proposed high gain dc-dc boost type converter

The parameters of proposed high gain dc-dc boost type converter were tabulated in table 5-4. Two used active-switches were STF20NM60D MOSFETs, the maximum voltage and current stresses of 600 V and 20 A, respectively. The isolated TLP250 amplifiers is used to drive for two active-switches. Six used power diodes were C3D20060D, the maximum voltage and current stresses are 600 V and 20 A, respectively.

Table 5-4 Parameters for experiment

Parameter		Value
Input voltage (V_{dc})		25 V - 100 V
Output voltage (V_o)		400 V
Output power		800 W
Mosfets (STF20NM60D)		20 A / 600 V
Diodes (C3D20060D)		20 A / 600 V
Inductors (f_{car})	L_1	700 μH / 20 A
	L_2	700 μH / 20 A
Capacitor (fref)	C_1	68 μF / 200 V
	C_0	220 μF / 450 V
Resistor load		200 Ω / 1 kW
Switching Frequency		20 kHz

1. Experimental results with voltage gain, G=8

Fig. 5-23 shows control gate signals for switches S_a and S_b with G=8. The control gate signal for switches S_b is the same duty cycle as the control gate signal for switches S_b. These signal are different phase of 180 as shown in Fig. 5-23.

Fig. 5-24 ~ 5-28 show the experimental results of the proposed high gain dc-dc boost type converter with G=8. As shown in Fig. 5-24, the output voltage is 400 V with the low input voltage of 50 V. The voltage of the C_1 and output current are 350 V and 2 A, respectively.

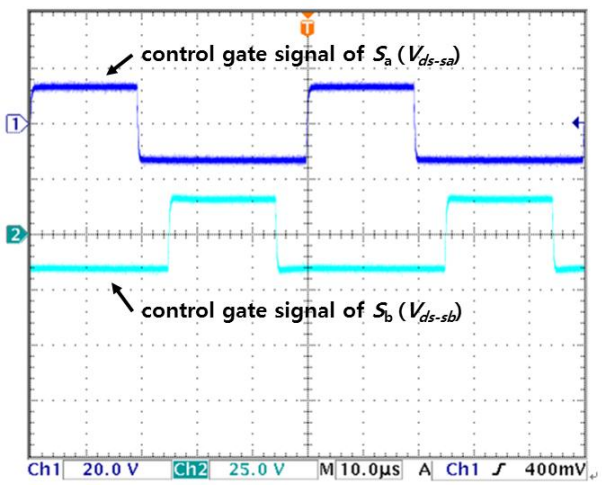

Fig. 5-23 Experimental waveforms of control gate signals of S_a - S_b when V_{dc}=50 V

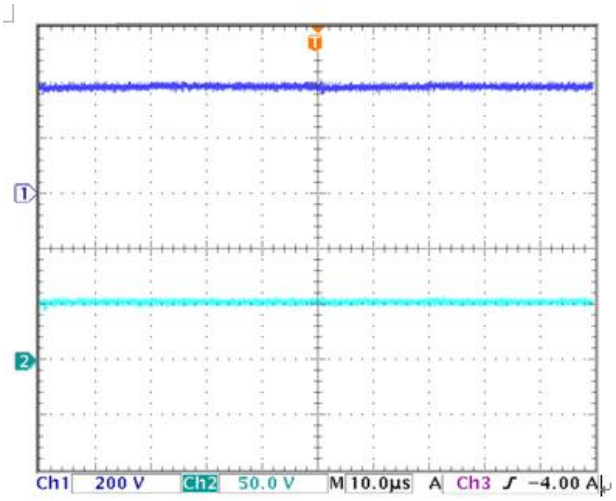

(a) Output voltage (V_o), input voltage (V_{dc})

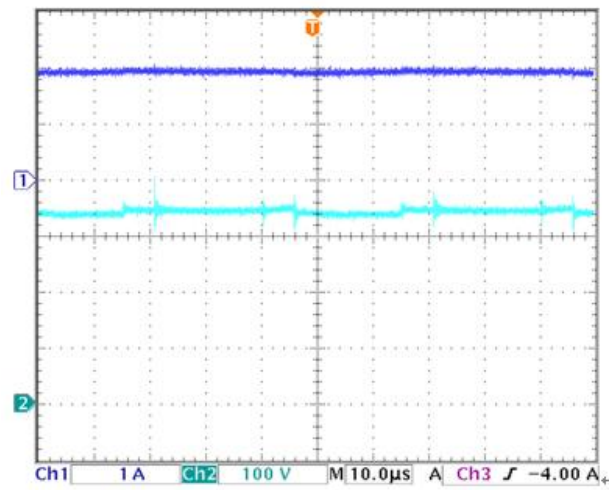

(b) Load current (I_o) and C_1 capacitor voltage (V_{c1})

Fig. 5-24 Experimental waveforms of the proposed converter when V_{dc}=50 V

Diode D_a voltage waveform, diode D_b voltage waveform, and diode D_c voltage waveform are the square waveform as shown in Fig. 5-25. The maximum voltage across the diode D_a and diode D_b are 150 V meanwhile that of diode D_c is 50 V. The maximum voltage across the diode D_3 is 350 V.

From Fig. 5-26, we can see that diode D_1 voltage, diode D_2 voltage, switch S_a voltage and switch S_b voltage also are the square waveform and are 350 V. The inductor L_1 current and inductor L_2 current are the same value and are 8 A.

As shown in Fig. 5-27, the current ripple on inductor L_1 and inductor L_2 are 2.8 A. The voltage across on the inductor L_1 current and inductor L_2 current are the same value. Fig. 5-28 shows the current wave form on diodes D_a, D_b and D_c. The current stress on diodes D_a, D_b and D_c is equal to the inductor current and are 9 A.

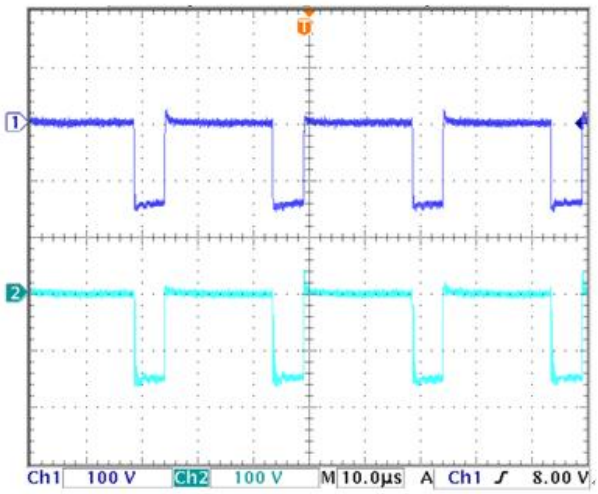

(a) Diode D_a voltage (V_{Da}), diode D_b voltage (V_{Db})

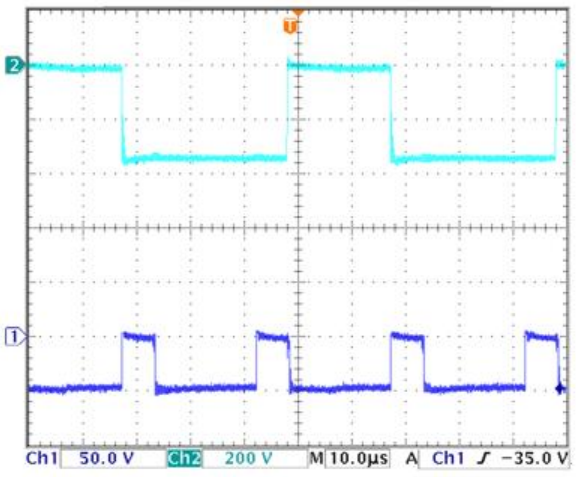

(b) Diode D_3 voltage (V_{D3}) and diode D_c voltage (V_{Dc})

Fig. 5-25 Experimental waveforms of the proposed converter when V_{dc}=50 V

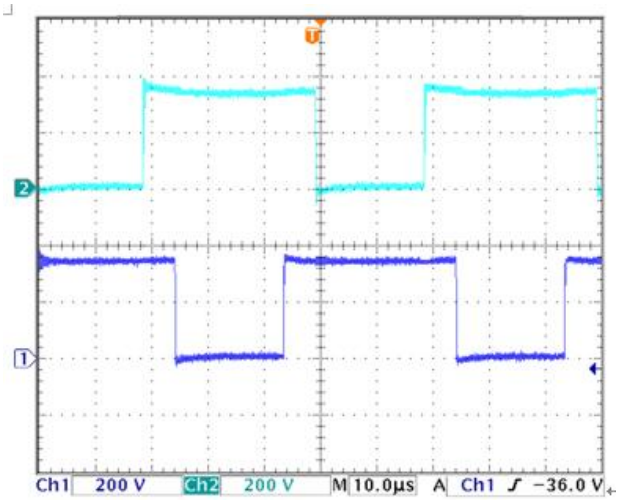

(a) Switch S_a voltage (V_{ds-sa}) and switch S_b voltage (V_{ds-sb})

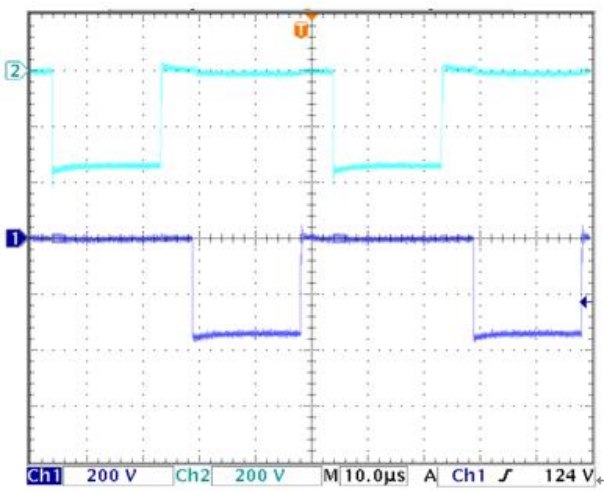

(b) Diode D_1 voltage (V_{D1}) and diode D_2 voltage (V_{D2})

Fig. 5-26 Experimental waveforms of the proposed converter when V_{dc}=50 V

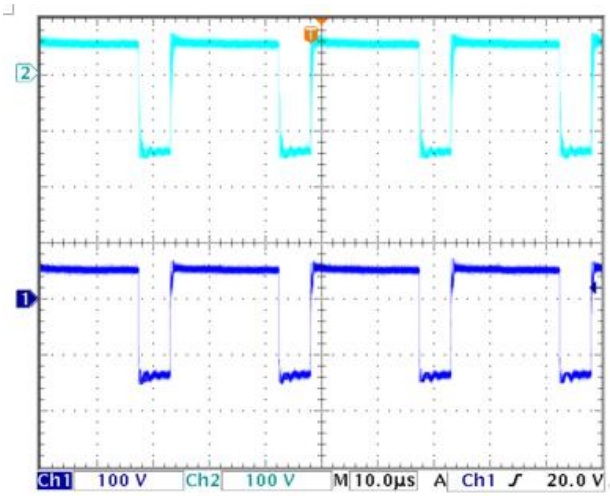

(a) Voltage across inductor L_1 (V_{L2}), and voltage across inductor L_2 (V_{L2}),

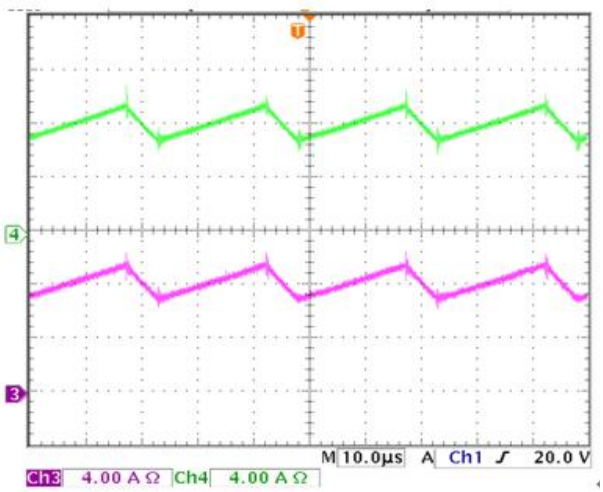

(b) Inductor L_1 current (i_{L2}), and inductor L_2 current (i_{L2}).

Fig. 5-27 Experimental waveforms of the proposed converter when V_{dc}=50 V

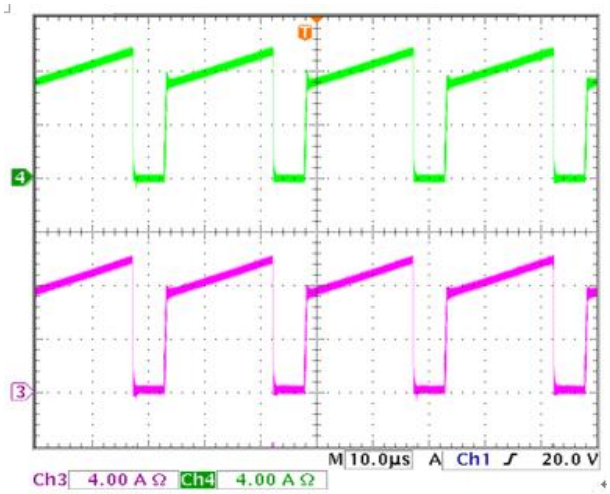

(a) Diode D_a current (i_{Da}), and diode D_b current (i_{Db})

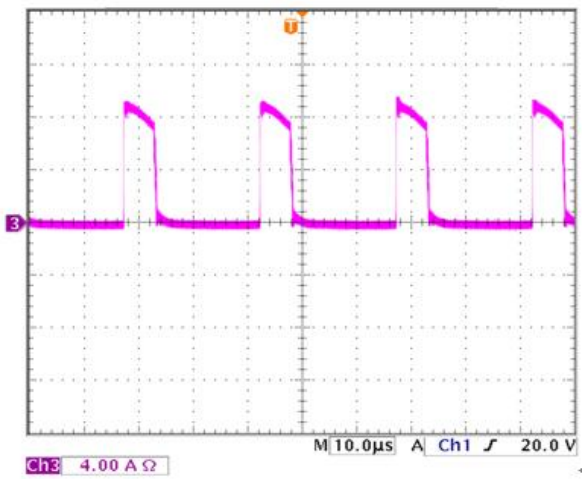

(b) Diode D_c current (i_{Dc})

Fig. 5-28 Experimental waveforms of the proposed converter when V_{dc}=50 V

2. Experimental results with voltage gain, G=4

Fig. 5-29 shows control gate signals for switches S_a and S_b with G=4. Similar to case of G=4, the control gate signal for switches S_b is the same duty cycle as the control gate signal for switches S_b. These signal are different phase of 180 as shown in Fig. 5-29. However, the duty cycle in case of G=4 is lower than the duty cycle in case of G=8.

Fig. 5-30 ~ Fig. 5-34 show the experimental results of the proposed high gain dc-dc boost type converter with G=4. As shown in Fig. 5-30, the output voltage is 400 V with the low input voltage of 100 V. The voltage of the C_1 and output current are 300 V and 2 A, respectively.

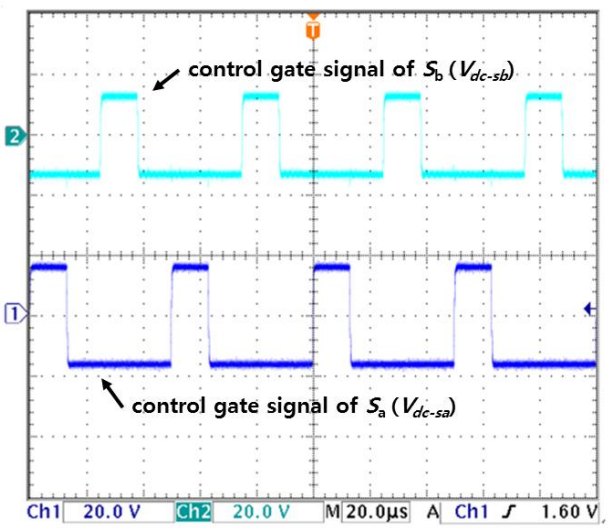

Fig. 5-29 Experimental waveforms of control gate signals of S_a-S_b when V_{dc}=100 V

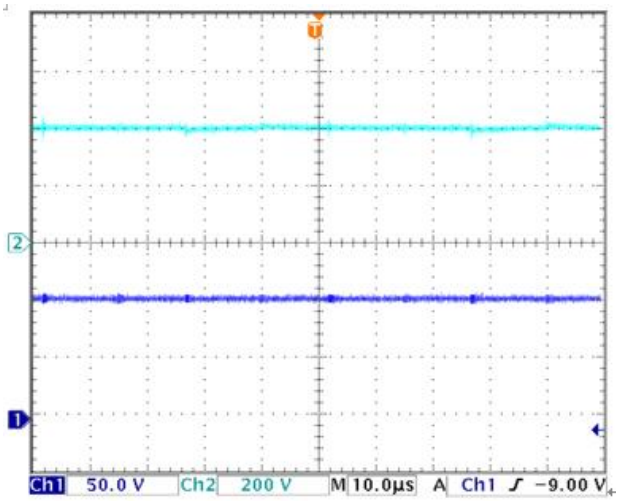

(a) Output voltage (V_0) and input voltage (V_{dc})

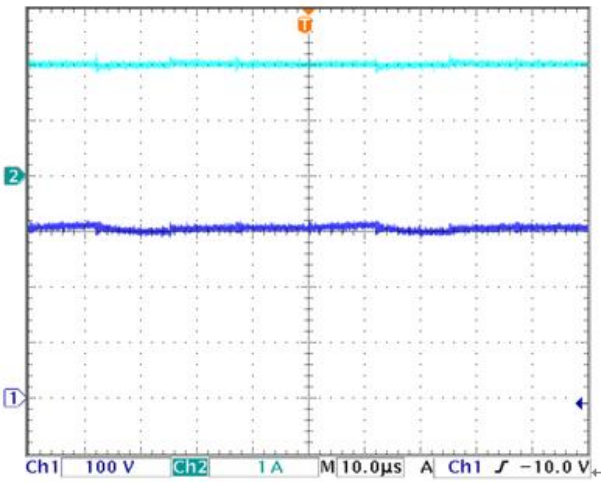

(b) Load current (I_o) and C_1 capacitor voltage (V_{c1})

Fig. 5-30 Experimental waveforms of the proposed converter when V_{dc}=100 V

Diode D_a voltage waveform, diode D_b voltage waveform, and diode D_c voltage waveform are the square waveformas shown in Fig. 5-31. The maximum voltage across the diode D_a and diode D_b are 100 V meanwhile that of diode D_c is 100 V. The maximum voltage across the diode D_3 is 300 V.

From Fig. 5-32, we can see that diode D_1 voltage, diode D_2 voltage, switch S_a voltage and switch S_b voltage also are the square waveform and are 300 V.

The inductor L_1 current and inductor L_2 current are the same value and are 4 A. As shown in Fig. 5-33, the current ripple on inductor L_1 and inductor L_2 are 2.4 A. The voltage across on the inductor L_1 current and inductor L_2 current are the same value. Fig. 5-34 shows the current waveform on Diodes D_a, D_b and D_c. The current stress on diodes D_a, D_b and D_c is equal to the inductor current and are 5.6 A.

Fig. 5-35 shows the dynamic performance of proposed high gain dc-dc boost type converter when $G=8$. In this case, resistor load is 200 Ω and input voltage changes from 0 V to 50 V. The output voltage reaches from 0 V to 400 V and the transient time is approximately 0.03 sec.

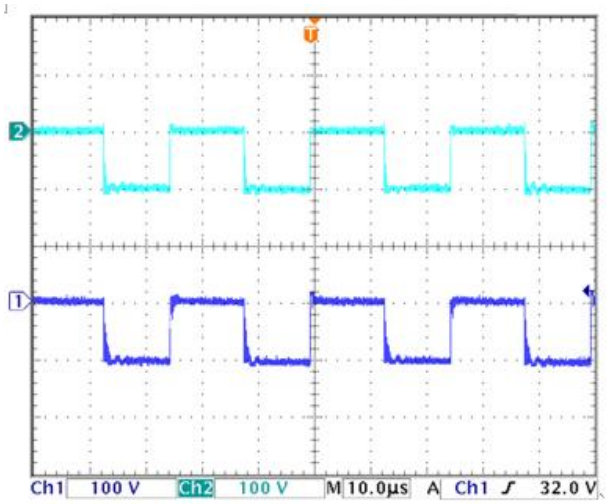

(a) Diode D_a voltage (V_{Da}) and diode D_b voltage (V_{Db})

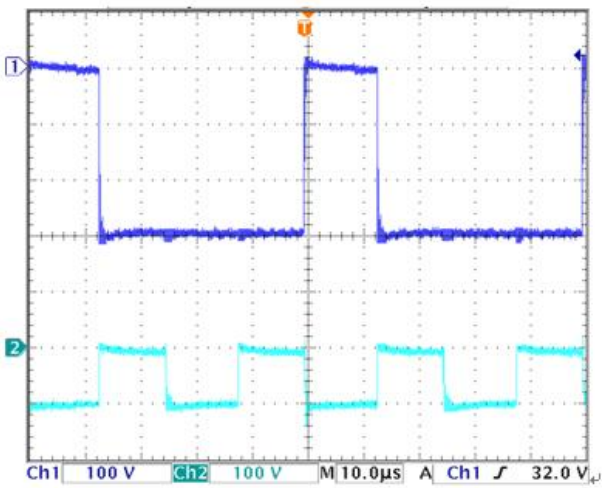

(b) Diode D_3 voltage (V_{Dc}) and diode D_c voltage (V_{D3})

Fig. 5-31 Experimental waveforms of the proposed converter when V_{dc}=100 V

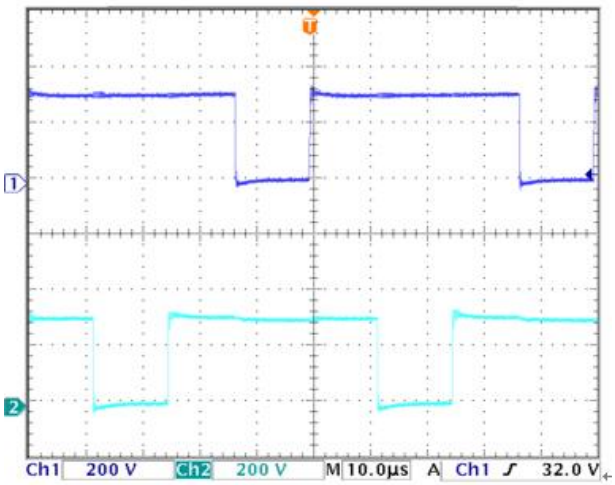

(a) Switch S_a voltage (V_{dc-sa}) and switch S_b voltage (V_{dc-sb})

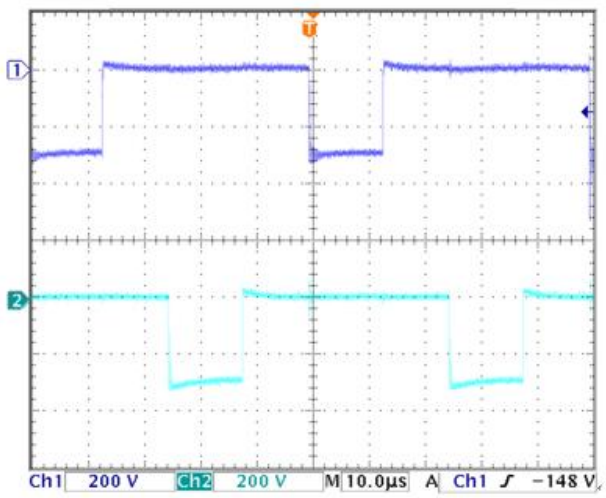

(b) Diode D_1 voltage (V_{D1}) and diode D_2 voltage (V_{D2})

Fig. 5-32 Experimental waveforms of the proposed converter when V_{dc}=100 V

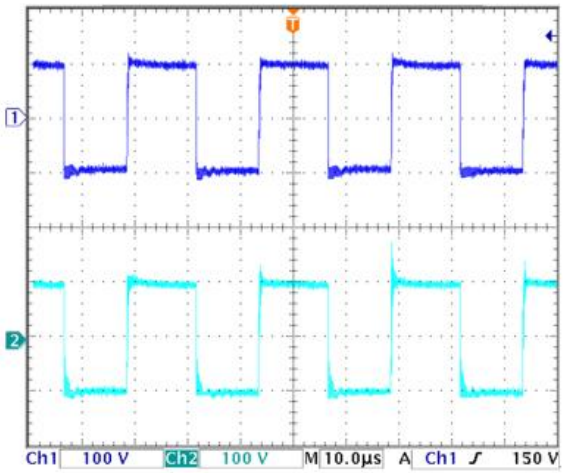

(a) Voltage across inductor L_1 (V_{L1}), and voltage across inductor L_2 (V_{L2})

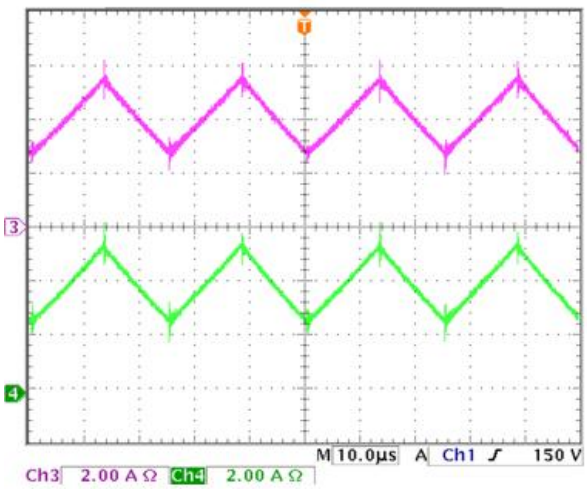

(b) Inductor L_1 current (i_{L1}), and inductor L_2 current (i_{L2})

Fig. 5-33 Experimental waveforms of the proposed converter when V_{dc}=100 V

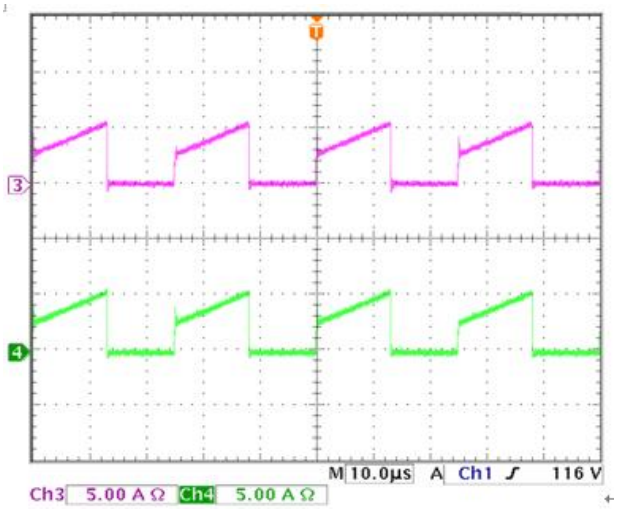

(a) Diode D_a current (i_{Da}), and diode D_b current (i_{Db})

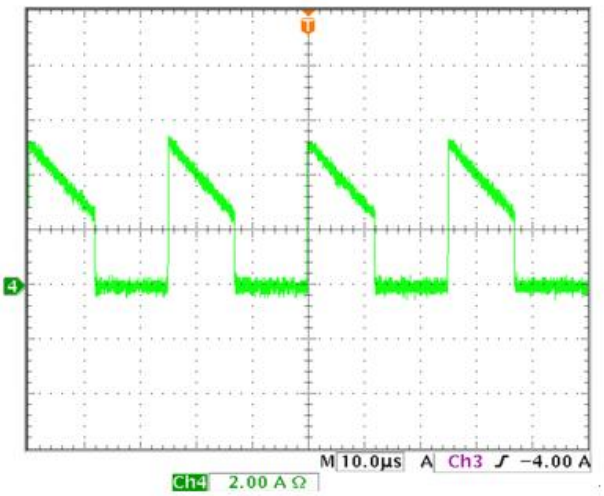

(b) Diode D_c current (i_{Dc})

Fig. 5-34 Experimental waveforms of the proposed converter when V_{dc}=100 V

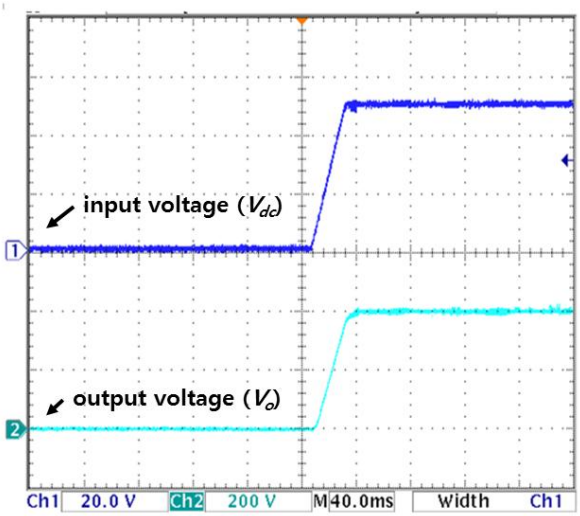

Fig. 5-36 Dynamic performance of proposed high gain dc-dc boost type converter

Ⅵ. Conclusions

The high gain boost converter topology is applicable to photovoltaic or fuel cells applications. This dissertation research has been focused on high gain dc-dc boost converter topology. The major conclusions from this research are summarized below:

1. A novel high gain dc-dc boost type converter using switched-inductor has been introduced. The proposed topology is based on the Switched-inductor structure. Compared to a classical boost for the same input and output voltage gain, the proposed topology could reduce voltage stress across semiconductors and capacitor. Besides that, a high voltage gain can be achieved with a small duty cycle. Therefore, the proposed high gain dc-dc boost type converter topology is suitable for high gain conversion applications where a varying low dc input voltage is converted to a high stabilized dc output voltage.

2. By adding one more witched-inductor cell into the proposed high gain dc-dc boost type converter using switched-inductor, the voltage gain of the proposed high gain dc-dc boost type converter using 2-switched-inductor cell can increase. Besides that, a high voltage gain can also be achieved with a small duty cycle.

3. The extension of the proposed high gain dc-dc boost type converter using switched-inductor was proposed. By adding n-Switched-inductor cells, the voltage gain of proposed topology can rise significantly.

In addition, the PWM modulation method of the proposed high gain dc-dc boost type converter using switched-inductor were presented. Circuit analysis, operating theories and a guideline of passive components selection of the proposed novel high gain dc-dc boost type converter are presented.

Simulation results of proposed converter using 1-switched-inductor cell and

proposed converter using 2-switched-inductor cells in PSIM software with 400V output voltage and 800W output power are shown to verify the theoretical analysis. Finally, The experiment prototype of the proposed high gain dc-dc boost type converter was developed based on kit TMS320F28035 (i.e., clocked at frequency of 60 MHz) of Texas Instruments was used to implement the PWM scheme. The experimental results of the proposed novel high gain dc-dc boost type converter are also indicated to verify calculated equations and theoretical analyses.

Contributions made in this study are:

- Power circuit implementation and design;
- Development of new high gain dc-dc boost type converter using 1-switched-inductor cell
- Development of new high gain dc-dc boost type converter using 2-switched-inductor cells.
- Development of new high gain dc-dc boost type converter topology using n-switched-inductor cells.
- Development of control algorithm for the proposed high gain dc-dc boost type converter.
- Guidelines for components design of proposed converter.
- Methods to issues on digital controller implementations are indicated.

ABSTRACT

A Study on the DC-DC Boost Type Converter using Switched-Inductor

Oh Man-Seok
Advisor : Prof. Cho Geum Bae, Ph.D.
Department of Electrical Engineering
Graduate School of Chosun University

The conventional boost converter topologies are not suitable for high gain conversion applications where a low dc input voltage is converted to a high stabilized dc output voltage. The other demerits of conventional dc-dc boost converter are high voltage stress across power semiconductor and a large inductance that is required to guarantee operating in continuous conduction mode. Recently, the high boost dc-dc scheme is one most of the topic that attracted the attention of researchers because they have some merits over the conventional boost converter. In this study, a novel high gain dc-dc boost type converter is discussed. The proposed structure is based on the switched-inductor structure. As a results, the high output voltage is boosted from the low input voltage and without using transformer. Compared to a classical boost for the same input and output voltage gain, the proposed topology could reduce voltage stress across semiconductors and capacitor. Besides that, a high voltage gain can be achieved with a small duty cycle. Therefore, the proposed high gain dc-dc boost type converter topology is suitable for high gain

conversion applications where a varying low dc input voltage is converted to a high stabilized dc output voltage. Circuit analysis, operating theories in the continuous conduction mode (CCM) and discontinuous conduction mode (DCM) of the proposed novel high gain dc-dc boost type converter are presented. Furthermore, the guideline of passive components selection of the proposed novel high gain dc-dc boost type converter is illustrated. Then, the proposed converter is extended to multi-switched inductor cell for high boost voltage achievement. Simulation results of proposed converter using 1-switched-inductor cell and proposed converter using 2-switched-inductor cells in PSIM software with 400V output voltage and 800W output power are shown to verify the theoretical analysis. A close-loop controller was used to simulate the dynamic respond for the proposed converter. Finally, the experiment prototype of the proposed high gain dc-dc boost type converter was built to verify the analysis. The kit DSP TMS320F28035 (i.e., clocked at frequency of 60 MHz) of Texas Instruments was used to implement the PWM scheme. The experimental results of the proposed novel high gain dc-dc boost type converter are also indicated to verify theoretical analyses and calculated equations.

Reference

[1] C. Muranda and et al., “Modified SEPIC dc-dc boost converter with high output-gain configuration for renewable applications”, Proc. IEEE Conference on Energy Conversion (CENCON),pp. 300-304, 2017.

[2] P. K. Maroti, and et al., “A high gain modified SEPIC dc-dc boost converter for renewable energy application”, Proc. IEEE Conference on Energy Conversion (CENCON),pp. 317-322, 2017.

[3] Zh. Qian, O. A. Rahman, and I. Batarseh, “An integrated four-port DC/DC converter for renewable energy applications,” IEEE Trans. Power Electron.,vol. 25, no. 7, pp. 1877 - 1887, Jul. 2010.

[4] N. Kato, K. Kurozumi, N. Susuld, and S. Muroyama, “Hybrid power supply system composed of photovoltaic and fuel-cell systems,” in Proc. Int. Telecommun. Energy Conf., pp. 631 - 635, 2001.

[5] K. Rajashekara, “Hybrid fuel-cell strategies for clean power generation,” IEEE Trans. Ind. Appl., vol. 41, no. 3, pp. 682 - 689, May/Jun. 2005.

[6] A.I.Bratcu, I. Munteanu, S. Bacha, D. Picault,and B.Raison,"CascadedDC - DCconverterphotovoltaicsystems:poweroptimizationissues,"IEEE Trans. Ind. Electron., vol. 58, no. 2, pp. 403-411, February 2011.

[7] H. Krishnaswami and N. Mohan, “Three-port series-resonant DC - DC converter to interface renewable energy sources with bidirectional load and energy storage ports,” IEEE Trans. Power Electron., vol. 24, no. 10, pp. 2289 - 2297, Mar. 2009.

[8] F. Z. Peng, H. Li, G. J. Su, and J. S. Lawler, “A new ZVS bidirectional dc - dc converter for fuel cell and battery application,” IEEE Trans. Power Electron.,vol. 19, no. 1, pp. 54 - 65, Jan. 2004.

[9] R. Gopinath, S. Kim, J. H. Hahn, P. N. Enjeti, M. B. Yeary, and J. W. Howze, “Development of a low cost fuel cell inverter system with DSP

control," IEEE Trans. Power Electron., vol. 19, no. 5, pp. 1256 - 1262, Sep. 2004.

[10] M. A. S. Masoum, H. Dehbonei, and E. F. Fuchs, "Theoretical and experimental analyses of photovoltaic systems with voltage and current-based maximum power-point tracking," IEEE Trans. Energy Convers.,vol. 17, no. 4, pp. 514 - 522, Dec. 2002.

[11] M. Durr, A. Cruden, S. Gair, and J. R. McDonald, "Dynamic model of a lead acid battery for use in a domestic fuel cell system," Elsevier J. Power Sources, vol. 161, no. 2, pp. 1400 - 1411, Oct. 2006.

[12] K. Jin, X. Ruan, M. Yang, and M. Xu, "A hybrid fuel cell power system," IEEE Trans. Power Del., vol. 56, no. 4, pp. 1212 - 1222, Apr. 2009.

[13] L. N. Khanh, J. J. Seo, Y. S. Kim, and D. J. Won, "Power-management strategies for a grid-connected PV-FC hybrid system," IEEE Trans. Ind. Electron.,vol. 25, no. 3, pp. 1874 - 1882, Jul. 2010.

[14] S. H. Hosseini, S. Danyali, F. Nejabatkhah, and S. A. K. Mozafari Niapour, "Multi-input DC boost converter for grid connected hybrid PV/FC/battery power system," in Proc. IEEE Elect. Power Energy Conf., pp. 1 - 6, 2010.

[15] Y. M. Chen, Y. Ch. Liu, and F. Y. Wu, "Multi-input DC/DC converter based on the multiwinding transformer for renewable energy applications," IEEE Trans. Ind. Electron.,vol. 38, no. 4, pp. 1096 - 1103, Jul./Aug. 2002.

[16] Hernandez J. C., Mira M. C., Sen G., Thomsen O. C., and Andersen M. A. E., "Isolated boost converter with bidirectional operation for super capacitor applications," J. Power Electronics, vol. 13, no. 4, pp. 507-515, July 2013.

[17] T. J. Liang, J. H. Lee, S. M. Chen, J. F. Chen, and L. S. Yang, "Novel

isolated high-step-up DC - DC converter with voltage lift," IEEE Trans. Ind. Electron.,vol. 60, no. 4, pp. 1483 - 1491, Apr. 2013.

[18] Zhe Zhang, Ziwei Ouyang, Ole C. Thomsen and Michael A. E. Andersen, "Analysis and Design of a Bidirectional Isolated DC-DC Converter for Fuel Cells and Super Capacitors Hybrid System," IEEE Transactions on Power Electronics,vol. 27, no. 2, pp. 848 - 859, 2012.

[19] R. J. Wai, Ch. Y. Lin, and Y. R. Chang, "High step-up bidirectional isolated converter with two input power sources," IEEE Trans. Ind. Electron.,vol. 56, no. 7, pp. 2629 - 2643, Jul. 2009.

[20] Jabbari, Masoud, H. Farzanehfard, and G. Shahgholian. "Isolated Topologies of Switched-Resonator Converters." Journal of Power Electronics,vol. 10, no. 2, pp. 125-131, Mar. 2010.

[21] W. Li, and X. He, "Review of non-isolated high-step-up dc/dc converters in photovoltaic grid-connected applications," IEEE Trans. Ind. Electron., vol. 58, no. 4, pp. 1239 - 1250, April 2011.

[22] W. Li, W. Li, X. Xiang, Y. Hu, and X. He, "High step-up interleaved converter with built-in transformer voltage multiplier cells for sustainable energy applications," IEEE Trans. Power Electron, vol. 29, no. 6, pp. 2829 - 2836, Jun. 2014.

[23] S. Padmanaban, A. Iqbal and H. Abu-Rub, "Implementation and control of extra high voltage dc-dc boost converter," Proc. IET Chennai Fourth International Conference on Sustainable Energy and Intelligent Systems (SEISCON 2013), pp.182-188, 2013.

[24] F. S. Garcia, J. A. Pomilio, and G. Spiazzi, "Modeling and control design of the interleaved double dual boost converter," IEEE Trans. Ind. Electron., vol. 60, no. 8, pp. 3283-3290, Aug. 2013.

[25] R. J. Wai and K. H. Jheng, "High-efficiency single-input multiple-output DC - DC converter," IEEE Trans. Power Electron., vol.

28, no. 2, pp. 886 - 898, Feb. 2013.

[26] L.S.Yang, T.J.Liang, and J.F.Chen, "Transformer-less DC - DC converter with high step-up voltage gain," IEEE Trans. Ind. Electron.,vol. 56, no. 8, pp. 3144 - 3152, Aug. 2009.

[27] X. Huang, X. Wang, T. Nergaard, J. S. Lai, X. Xu, and L. Zhu, "Parasitic ringing and design issues of digitally controlled high power interleaved boost converters," IEEE Trans. Power Electron., vol. 19, no. 5, pp. 1341 - 1352, Sep. 2004.

[28] Y. Ch. Liu and Y. M. Chen, "A systematic approach to synthesizing multi-input DC - DC converters," IEEE Trans. Power Electron.,vol. 24, no. 1, pp. 116 - 127, Jan. 2009.

[29] L. Yan, R. Xinbo, Y. Dongsheng, L. Fuxin, and C. K. Tse, "Synthesis of multiple-input DC/DC converters," IEEE Trans. Power Electron.,vol. 25, no. 9, pp. 2372 - 2385, Sep. 2010.

[30] A. Kwasinski, "Identification of feasible topologies for multiple-input DC - DC converters," IEEE Trans. Power Electron.,vol. 24, no. 3, pp. 856 - 861, Mar. 2010.

[31] H. Matsuo, W. Lin, F. Kurokawa, T. Shigemizu, and N. Watanabe, "Characteristics of the multiple-input DC - DC converter," IEEE Trans. Ind. Electron.,vol. 51, no. 3, pp. 625 - 631, Jun. 2004.

[32] H. Tao, A. Kotsopoulos, J. L. Duarte, and M. A. M. Hendrix, "Family of multiport bidirectional DC - DC converters," in Proc. IEE Elect. Power Appl., pp. 451 - 458,2006.

[33] L. Solero, A. Lidozzi, and J. A. Pomilio, "Design of multiple-input power converter for hybrid vehicles," IEEE Trans. Power Electron., vol. 20, no. 5, pp. 1007 - 1016, Sep. 2005.

[34] A. Khaligh, J. Cao, and Y. J. Lee, "A multiple-input DC - DC converter topology," IEEE Trans. Power Electron., vol. 24, no. 3, pp. 862 - 868,

Mar. 2009.

[35] A. Di Napoli, F. Crescimbini, F. G. Capponi, and L. Solero, "Control strategy for multiple input dc - dc power converters devoted to hybrid vehicle propulsion system," in Proc. IEEE Int. Symp. Ind. Electron., L'Aquila, Italy, pp. 1036 - 1041, 2002.

[36] Moises Tanca V. and Ivo Barbi, "Nonisolated High Step-up Stacked DC-DC Converter Based on Boost Converter Elements for High Power Application", in Proc. IEEE International Symposium on Circuits and Systems (ISCAS), pp.249-252, 2011.

[37] B. Axelrod, Y. Berkovich, and A. Ioinovici, "Switched-capacitor/switched-inductor structures for getting transformerless hybrid dc-dc PWM converters," IEEE Trans. Circuits Syst. I, Reg. Papers, vol. 55, no. 2, pp. 687-696, March 2008.

[38] B. Axelrod, Y. Beck, and Y. Berkovich, "High step-up dc - dc converter based on the switched-coupled-inductor boost converter and diode-capacitor multiplier: steady state and dynamics," IET Power Electron.,vol. 8, no. 8, pp. 1420 - 1428, 2015.

[39] J. baby and D. David, "High gain single switch boost converter for sustainable energy applications using switched capacitor and coupled inductor", Proc. International Conference on Electrical, Electronics, and Optimization Techniques (ICEEOT), pp. 727-731,2016.

[40] Y. P. Hsieh, J. F. Chen, T. J. Liang, and L. S. Yang, "Novel high step-up DC-DC converter with coupled-inductor and switched-capacitor techniques," IEEE Trans. Ind. Electron.,vol. 59, no. 2, pp. 998 - 1007, Feb. 2012.

[41] H. Liu, H. Hu, H. Wu, Y. Xing, and I. Batarseh, "Overview of high-step-up coupled-inductor boost converters," IEEE J. Emerg. Sel. Topics Power Electron.,vol. 4, no. 2, pp. 689 - 704, June 2016.

[42] Y. P. Siwakoti, F. Blaabjerg, and P. C. Loh, “High step-up trans-inverse (Tx－1) DC－DC converter for the distributed generation system,” IEEE Trans. Ind. Electron.,vol. 63, no. 7, pp. 4278－4291, July 2016.

[43] Y. Jiao, F.L. Luo, and M. Zhu, “Voltage-lift-type switched-inductor cells for enhancing DC－DC boost ability: principles and integrations in Luo converter,” IET Power Electron., vol. 4, no. 1, pp. 131-142, Jan. 2011.

[44] G. Wu, X. Ruan, and Z. Ye, "Non-isolated high step-up DC－DC converters adopting switched-capacitor cell," IEEE Trans. Ind. Electron.,vol. 62, no. 1, pp. 383-393, Jan. 2015.

[45] L. S. Yang, T. J. Liang, and J. F. Chen, “Transformerless DC-DC converters with step up voltage gain,” IEEE Trans. Ind. Electron.,vol. 56, no. 8, pp. 3144-3152, Aug. 2009.

[46] Y. Tang, D. Fu, T. Wang, and Z. Xu, "Hybrid switched-inductor converters for high step-up conversion," IEEE Trans. Ind. Electron., vol. 62, no. 3, pp. 1480－1490, Mar. 2015.